Structural, functional and stability characterisation of human glutathione *S*-transferase Pi

Donald Mhlanga

A dissertation submitted to the Faculty of Science, University of the Witwatersrand, Johannesburg, in fulfilment of the requirements in fulfilment of the degree for Master of Science.

October 2018

Declaration

I, **Donald Mhlanga** (**587777**), am a student registered for the degree of **MSc** in the academic year **2018**.

I hereby declare the following:

 I am aware that plagiarism (the use of someone else's work without their permission and/or without acknowledging the original source) is wrong.

 I confirm that the work submitted for assessment for the above degree is my own unaided work except where explicitly indicated otherwise and acknowledged. In this context, I understand that the use of editing services is considered aided work and must be declared.

 I have not submitted this work before for any other degree or examination at this or any other University.

 The information used in the Dissertation **HAS NOT** been obtained by me while employed by, or working under the aegis of, any person or organisation other than the University.

 I have followed the required conventions in referencing the thoughts and ideas of others.

 I understand that the University of the Witwatersrand may take disciplinary action against me if there is a belief that this is not my own unaided work or that I have failed to acknowledge the source of the ideas or words in my writing.

Signature  on this **30th** day of **October, 2018**

Donald Mhlanga

Abstract

Glutathione *S*-transferases (GSTs) are Phase II detoxification enzymes that catalyse the conjugation of glutathione (GSH) to non-polar xenobiotic compounds to form water-soluble metabolites. Despite the low level of sequence similarity, the different GST classes follow the same canonical fold. hGSTP1-1 belongs to the Pi class and is involved in detoxification, as well as other non-classical roles such as regulating the MAP kinase pathway, protecting cells from nitrosative stress and regulating the function of 1-Cys peroxiredoxin. The structure, function and stability of GSTP1-1 was characterised to gain a better understanding of the general characteristics of the enzyme. The heterologous expression of hGSTP1-1 in *Escherichia coli* produces high yields of the enzyme that is then purified using immobilised metal affinity chromatography. A GSH-CDNB conjugation assay shows that the enzyme catalyses this reaction with a specific activity of 55.5 µmol/min/mg. The enzyme also binds 8-anilinonaphthalene-1-sulfonic acid (ANS), resulting in a blue shift and a two-fold increase in the fluorescence intensity of ANS. Far-UV circular dichroism shows that hGSTP1-1 is a predominantly alpha-helical protein, while intrinsic fluorescence studies show that the enzyme has Trp residues. Studies done using size exclusion HPLC show that the protein adopts a monomeric structure when exposed to high salt concentrations. Thermal unfolding of hGSTP1-1 shows that the enzyme unfolds irreversibly when exposed to increasing temperatures. Urea denaturation of the enzyme follows a two-state model ($N_2 \leftrightarrow 2U$) and shows that domain 1 and domain 2 unfold in a cooperative manner.

AKNOWLEGDEMENTS

Prof H.W. Dirr for his support and guidance throughout this project, and for giving me the opportunity to work in his lab.

Dr I.A. Achilonu for his supervision and guidance.

Prof R. Veale for his support.

All members of the Protein Structure-Function Research Unit.

The National Research Foundation and Wits PGMA for financial assistance.

My friends and family for their patience and unwavering support.

TABLE OF CONTENTS

LIST OF FIGURES

LIST OF TABLES

LIST OF ABBREVIATIONS

1-CysPrx	1-Cys peroxiredoxin
aiPLA2	acidic calcium-independent lysosomal phospholipase A2
ANS	8-anilinonaphthalene-1-sulfonic acid
AP-1	activator protein-1
BCNU	*N,N′*-bis(2-chloroethyl)-*N*-nitrosourea
BLAST	Basic Local Alignment Search Tool
CD	Circular Dichroism
CDNB	1-chloro-2,4-dinitrobenzene
DTNB	5,5'-dithio-bis-(2-nitrobenzoic acid)
DTT	dithiothreitol
EDTA	ethylene diamine tetracetic acid
GS^-	thiolate anion of glutathione
GSH	reduced glutathione
GSNO	*S*-nitrosoglutathione
hGSTP1-1	human glutathione *S*-transferase Pi
IC_{50}	half maximal inhibitory concentration
IMAC	immobilised metal affinity chromatography
IPTG	isopropyl β-D-1-thiogalactopyranoside
JNK	cJun N-terminal kinase
LPLA2	lysosomal phospholipase A2
MAPK	mitogen-activated protein kinase
MBP	maltose-binding protein
NO	nitric oxide
NOS	nitric oxide synthase
OD	optical density
SDS-PAGE	sodium dodecyl sulfate polyacrylamide gel electrophoresis
SE-HPLC	size exclusion high performance liquid chromatography
UPGMA	Unweighted Pair Group Method with Arithmetic Mean
UV	ultraviolet

CHAPTER 1
INTRODUCTION AND LITERATURE REVIEW

1.1 Brief background on glutathione *S*-transferases

Living organisms are constantly exposed to foreign chemicals such as plant phenols, aflatoxins and reactive oxygen species that can have toxic effects on the organism. There is therefore a need for biochemical protection mechanisms such as catalytic biotransformation against such toxic chemical species. Glutathione *S*-transferases (GSTs; EC 2.5.1.18) are a family of phase II detoxification enzymes that are mainly found in the cytosol (Mannervik *et al*., 1992). Phases I and II detoxification generally relates to the modification of lipophilic, apolar xenobiotic compounds into products that are polar and consequently less harmful to an organism (Rushmore and Tony Kong, 2002). GSTs mainly catalyse the conjugation of the endogenous water-soluble substrate glutathione (GSH) to electrophilic compounds through thioether linkages (Boyland and Chasseaud, 1967). This reaction is normally followed by phase III of detoxification, which involves the elimination of the conjugation products from the cell by an ATP-dependant glutathione *S*-conjugate export (GS-X) pump (Ishikawa, 1992), a multispecific organic anion transporter (Heijn *et al*., 1992), P-glycoprotein (Gottesman and Pastan, 1993), the multidrug-resistance-associated protein (Jedlitschky *et al.*, 1994; Kavallaris, 1997) or a broad-specificity anion transporter of dinitrophenol S-GSH (Saxena *et al*., 1992). GSTs have other non-classical roles in addition to their catalytic roles and ligandin function, such as the management of *S*-glutathiolated proteins that are generated as a result of oxidative stress (Hill *et al.*, 2010); the development of resistance to chemotherapeutic agents (Kodym *et al.*, 1999); the modulation of cell signalling pathways that influence apoptosis and cell proliferation (Voehringer *et al.*, 2000); and the biosynthesis and metabolism of leukotrienes (Shimizu *et al.*, 1990), prostaglandins (Uchida, 2000) and steroids (Platz and Giovannucci, 2004).

1.2 Structure of glutathione *S*-transferases

There is at least a 60% sequence similarity within a GST class and less than 30% similarity across the different classes, even though their overall architecture is similar (Dirr *et al*., 1994). GST structures are divided into the Alpha, Delta, Epsilon, Mu, Pi, Omega, Theta, Sigma and Zeta classes on the basis of their activity (Mannervik *et al*., 1985), structure (Hayes and Pulford, 1995), substrate specificities (Mannervik *et al*., 1985) and inhibitor sensitivities (Dirr *et al.*,

1994). A phylogenetic tree showing the relationships between different GST classes is shown in Figure 1.1. The primary sequence of the N-terminus within classes is better conserved than other regions of the protein since it includes an essential part of the active site (Dirr *et al.*, 1994). The N-terminal region of the enzyme contains a catalytically essential cysteine, serine or tyrosine residue that binds to the thiol group of GSH, thus lowering the pK_a from around 9 to approximately 6-7 in order to facilitate the conjugation reaction (Liu *et al.*, 1992; Atkins *et al*., 1993).

Most cytosolic GSTs are dimeric proteins that have a wide variety of properties involving the binding of ligands in addition to their catalytic function in the detoxification of xenobiotic compounds (Ketley *et al.*, 1975). Each subunit of the dimer (Figure 1.2) has two domains: a thioredoxin-like domain that consists of the GSH-binding site (G-site) and another domain made up of only α-helices which contains the hydrophobic binding site (H-site) (Reinemer *et al.*, 1992; Sinning *et al.*, 1993; Wang *et al*., 2009). Figure 1.3 shows the structure of GSTP1-1 with GSH bound the G-site. Despite the low level of sequence similarity, the structures of the different GSTs follow a comparable canonical fold. The N-terminal thioredoxin-like domain 1 (approximately residues 1-80) is connected to domain 2 (approximately residues 87-210) on the C-terminus by a short linker sequence (Dirr *et al*., 1994). Bonds that are formed at the dimer interface are important for the assembly and stability of the dimer, and often occur between subunits from the same class (Dirr *et al.*, 1994; Rossjohn *et al.*, 1998).

1.3 Glutathione *S*-transferase Pi

Class pi GSTs are a multigenic family of proteins that are related to GST Mu and to a lesser extent to GST Alpha (Hayes and Pulford, 1995). Figure 1.4 shows the similarities between the structures of human GST and rat GST Mu. Unlike the other GST classes which require GSH for isomerisation reactions, studies have shown that GSTP1-1 catalyses an isomerisation reaction that produces all-*trans*-retinoic acid from 13-*cis*-retinoic acid in the absence of GSH (Chen and Juchai, 1998).

1.3.1 Subcellular localisation of GSTP1-1

GSTP1-1 is mainly expressed in the cytosol of placenta, brain, lung, heart and liver cells (Strange *et* al., 1985; Guthenberg *et al*., 1986; Faulder *et al*., 1987). However, the enzyme is also found in the nuclei of human cancer cells where it prevents peroxide-induced DNA damage (Kobayashi, 1999, Kamada *et al*., 2004). A mushroom lectin which inhibits nuclear transport has been shown to inhibit the nuclear transfer of GSTP1-1, which suggests that there

is a specific transport system which is responsible for the transfer of the enzyme to the nucleus (Goto *et al*., 2009). There is also experimental data which suggest that the protein is localised in the mitochondria (Gallagher *et al*., 2006; Goto *et al.*, 2009).

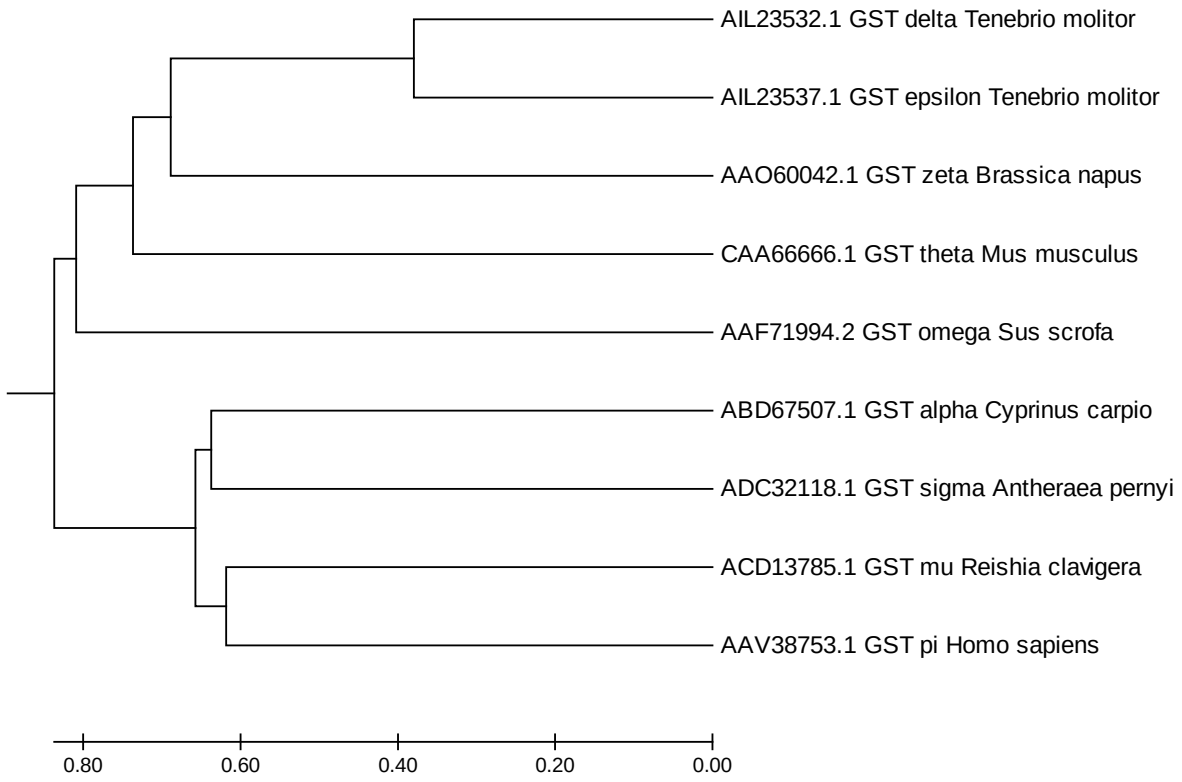

Figure 1.1: A phylogenetic tree showing the different glutathione *S*-transferase classes. The evolutionary history of the proteins belonging to the different GST classes in the different species was inferred using the Unweighted Pair Group Method with Arithmetic Mean (UPGMA) method. The optimal tree which is shown has a sum of branch length of 6.20178423. The phylogenetic tree which is shown is drawn to scale, and the branch lengths mimic the evolutionary distances used to infer the tree. The evolutionary distances were calculated using the Poisson correction method. All positions containing gaps and missing data were eliminated. All evolutionary analyses were performed in MEGA7 (Kumar *et al.*, 2016).

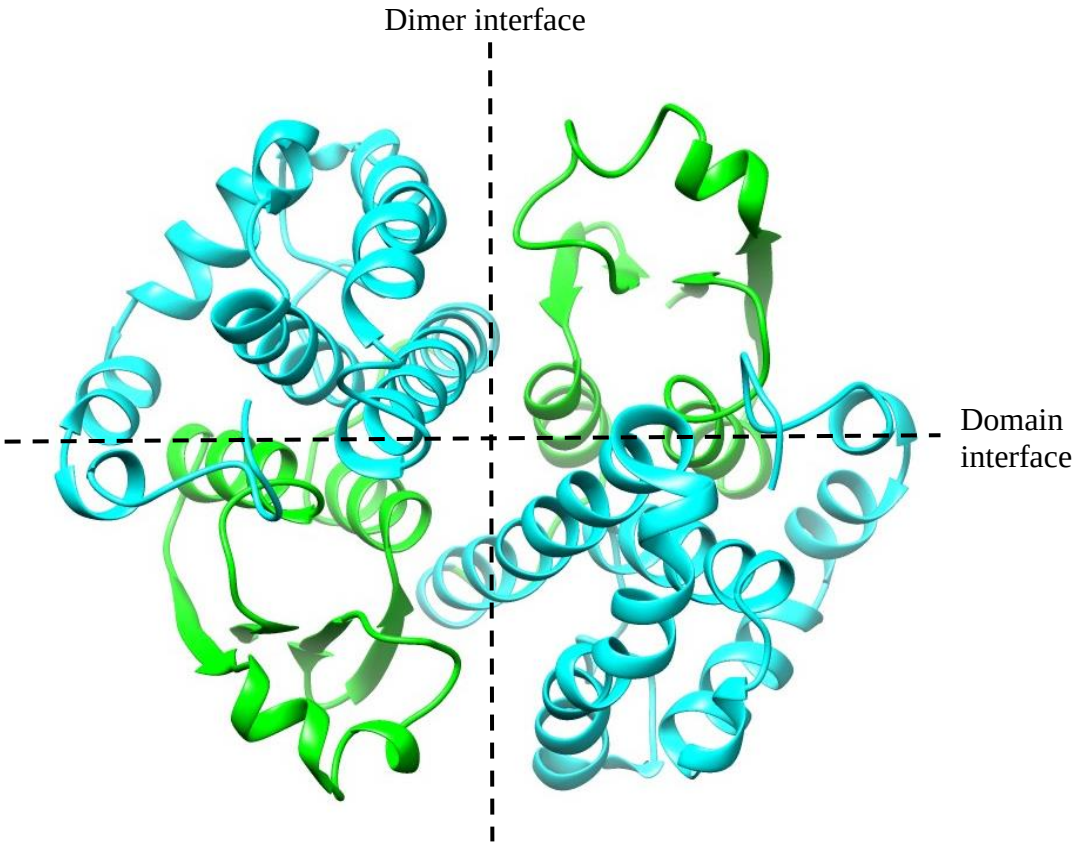

Figure 1.2: A crystal structure of human glutathione *S*-transferase Pi highlighting the dimer interface and the domain interface (PDB: 1GSY). The homodimeric enzyme has a molecular mass of 47 kDa. Each subunit of the dimer has two domains: a thioredoxin-like domain which contains the GSH-binding site (green) and a domain made up of only α-helices which contains the hydrophobic binding site (cyan). UCSF Chimera (Pettersen *et al.*, 2004) was used to create the image of the crystal structure.

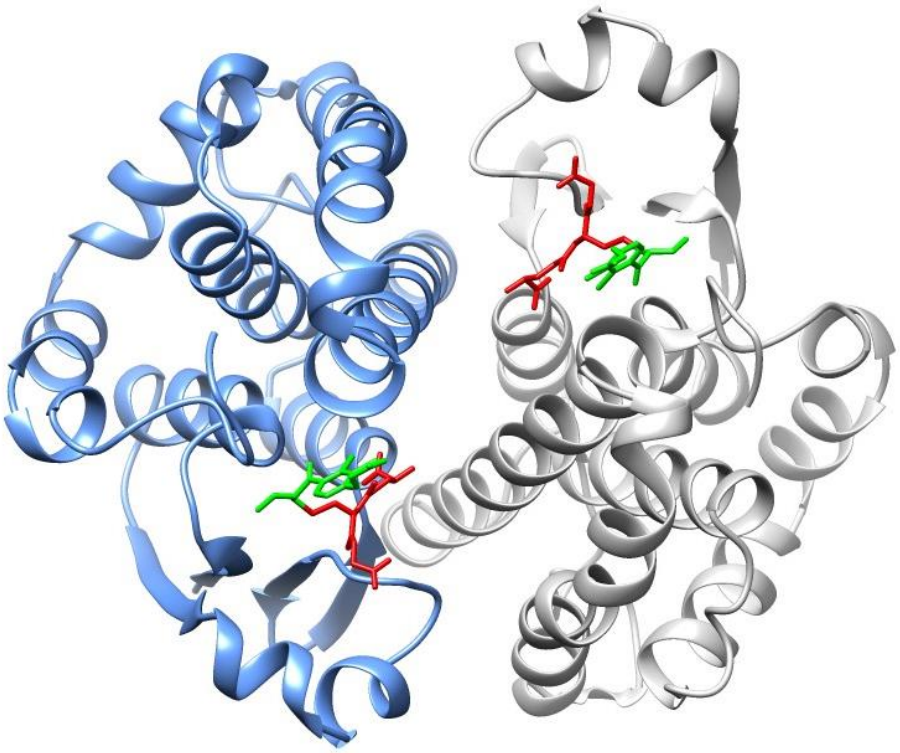

Figure 1.3: The dimeric structure of GSTP1-1 bound to glutathione (GSH) and ethacrynic acid (PDB: 3GSS). The two subunits that form the dimer are shown in blue and grey, respectively. GSH molecules (red) are bound to the G-site, while the two ethacrynic acid molecules (green) are bound to the H-site in each subunit. The G-site is located in the thioredoxin-like N-terminal domain, while the H-site is located in the C-terminal domain. UCSF Chimera (Pettersen *et al*., 2004) was used to create the image of the crystal structure.

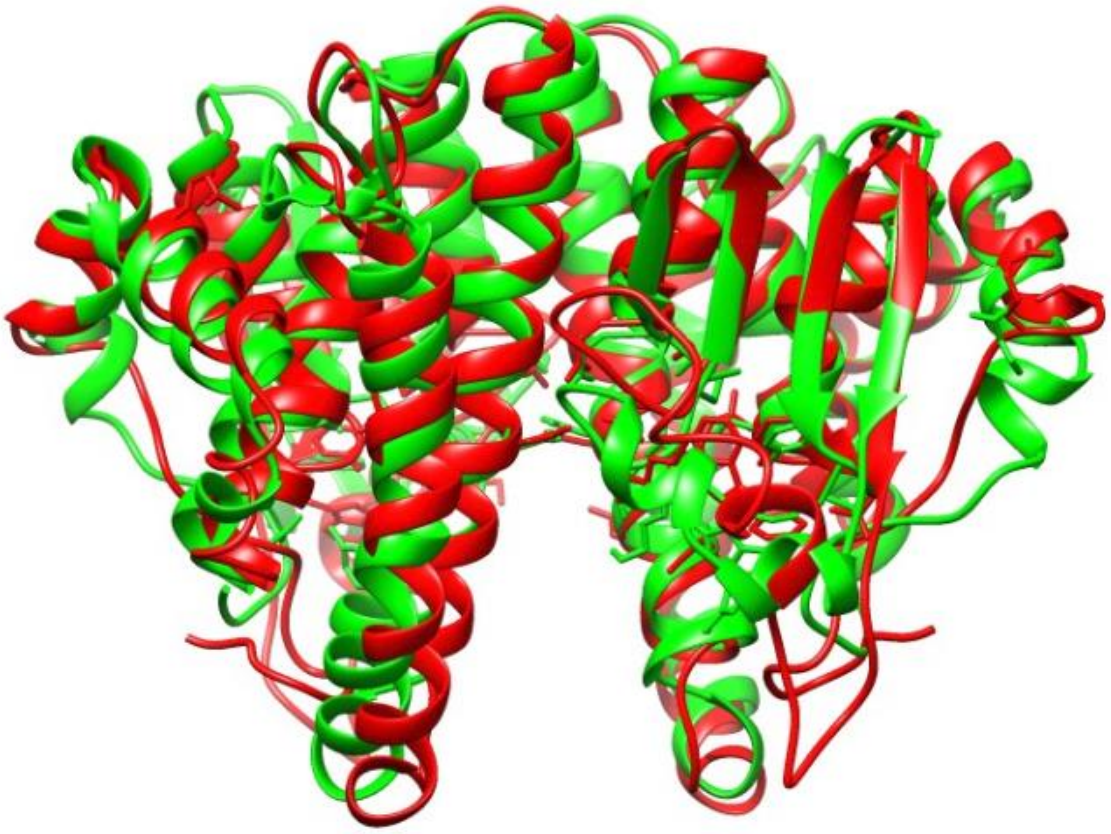

Figure 1.4: A comparison between the structures of GST Pi (green) and GST Mu (red). Human GSTP1-1 (PDB: 5X79) and rat GST-M1 (PDB: 6GSV) were aligned using UCSF Chimera. The two structures have very similar folds and the superposition has an RMSD of 1.91 Å, even though there is only 19.82% sequence identity between them. UCSF Chimera (Pettersen *et al*., 2004) was used to create the image of the crystal structure.

1.3.2 Structure and polymorphisms of GSTP1-1

The pi, mu and alpha GST classes share conservative motifs and conserved amino acid residues (Sinning *et al.*, 1993; Dirr *et al*., 1994) which have important roles in the manner in which the protein interacts with other proteins. These similarities also influence the mobility of the different elements that make up the protein (Sternberg *et al*., 1998), the lock-and-key motif which contributes to the function of the enzyme as a catalyst (Stenberg *et al.*, 2000; Alves *et al*., 2006), the substrate binding motif (Banham *et al.*, 2007) and the hydrophobic staple that influences protein folding (Stenberg *et al*., 2000). Tyr50 in GSTP1-1 acts as a 'key' stretching from the loop that comes before *β*-3 which fits into a hydrophobic 'lock' which is formed by the helices *α*-4 and *α*-5 in the second subunit of the homodimer. The protein also has a Tyr residue in *β*-1 which is in close proximity to the thiol group of GSH for the formation of hydrogen bonds (Sinning *et al*., 1993). A SNAIL/TRAIL (Ser-Asn-Ala-Ile-Leu/Thr-Arg-Ala-Ile-Leu) motif in the *α*-3 helix of domain 1 includes important residues that also contribute to the GSH binding site (Koonin *et al.,* 1994).

Human GSTP1-1 has polymorphic sites at codon 105 of exon 5 where a transition from an adenosine to a guanine causes an Ile(105)Val substitution in helix 4, and at codon 114 of the same exon which results in an Ala(114)Val substitution in helix 5 (Ali-Osman *et al.,* 1997). This gives rise to the three naturally occurring alleles, *hGSTP1-1∗A*, *hGSTP1-1∗B* and *hGSTP1-1∗C*. The allele labelled *A* has isoleucine at location 105 and alanine at location 114, the *B* allele has valine at location 105 and alanine at location 114, while the *C* allele has valine in both the 105 and 114 positions (Board *et al.,* 1989; Ahmad *et al.,* 1990; Ali-Osman *et al.,* 1997). The amino acid residue at position 105 is located in the middle of the active site of the enzyme, while residue 114 is situated at the start of helix-5 which is situated outside the H-site. Individuals with the Val at position 105 exhibit a much lower enzyme activity, are less efficient in detoxification (Zimniak *et al.,* 1994) and are more vulnerable to neoplasms (Oude *et al.,* 2003; Tempfer *et al.,* 2004; Ates *et al.,* 2005). The effect of the Ala(114)Val substitution is unclear, although the size and hydrophobicity of this residue may function as a determining factor of the substrate specificity of different isozymes (Hu *et al.,* 1999).

1.4 Factors influencing the stability of GST-P1

An understanding of the stability of protein molecules is important in structural biology, since it makes it possible to optimise their expression, purification, storage and structural characterisation. High levels of conformational disorder exist in protein molecules, which

allows for plasticity and flexibility of the protein. Some of the intrinsic factors that affect the structure of hGSTP1-1 include the presence of a stabilising Ile105 at the H-site, dimerisation and the presence of a hydrophobic staple motif. Other factors include binding of substrates to the active site of the enzyme and *S*-Nitrosation.

1.4.1 Ile105 in the H-site

Studying the three dimensional structure of hGSTP1-1 bound to *S*-hexylglutathione (Reinemer *et al.,* 1992) shows that Ile105 is adjacent to Tyr109, which allows for direct contact between the two amino acid residues facilitated by van der Waals forces. Modifying the bulkiness and hydrophobicity of the amino acid at position 105 affects the function of the structurally conserved Tyr109 which has a multifunctional role in the catalytic mechanism of the enzyme (Johansson *et al.,*1998). The analysis of crystals of hGSTP1-1 bound to the product of the conjugation reaction between GSH and ethacrynic acid (Oakley *et al.,* 1997), and kinetic studies involving the Y109F mutant of hGSTP1-1 using ethacrynic acid as a hydrophobic substrate (Lo Bello, *et al.,* 1997) have shown that the reaction between GSH and ethacrynic acid is assisted by the hydroxyl group of Tyr109 which stabilises the enolate intermediate.

Since hydrophobic interactions are mainly responsible for stabilising the folded configuration of protein molecules, substitutions that decrease or increase the hydrophobicity of amino acid side chains are likely to have an effect on the stability of hGSTP1-1. Substitutions such as Ile to Val that lower the hydrophobicity of the amino acid side chains that are located in the interior of the protein generally destabilise protein molecules due to the loss of favourable van der Waals interactions (Takano *et al.,* 1997). However, substituting small residues with larger ones that drastically increase the size of the side-chain also destabilises protein molecules due to the interruption of interactions with neighbouring residues, unfavourable steric contacts and the introduction of torsional strain (Takano *et al.,* 1995). The addition of bulkier amino acids (except Trp) to position 105 of hGSTP1-1 increases the thermal stability of the enzyme (Johansson *et al*., 1998), most likely as a result of the contribution of hydrophobic interactions introduced by the supplementary methylene groups.

1.4.2 The hydrophobic staple motif

The amino acid sequence governs the folded conformation that is eventually adopted by a protein molecule. Protein folding models have shown that a critical role is played by local associations that lower the structural flexibility at particular points of the polypeptide chain and therefore determine the pathway that will be followed during protein folding (Abkevich *et al.,*

1994; Bryngelson *et al.,* 1995; Li *et al.,* 1996). There are two local motifs at the N-terminus of α-helices that stabilise the secondary structural element and assist with the folding of the protein. The first one is an N-capping box that concerns the formation of reciprocal hydrogen bonds between the Ncap (Ser/Thr) and the N3 (Glu/Asp) residues of the helix (Presta and Rose, 1988; Richardson and Richardson, 1988), and the second one is a hydrophobic staple motif (Munoz *et al.,* 1995; Munoz and Serrano, 1995) which requires a hydrophobic association that is established between residues situated at the N' and N4 positions (using the nomenclature: N''-N'-Ncap-N1-N2-N3-N4; where N1-N4 are inside the helix and Ncap represents the borderline residue). Studies have shown that in GSTP1-1, there is a hydrophobic association between the α6-helix residue N4 (Tyr154) and the side chain of the loop residue N' (Ile149) which favours the correct conformation of the α6-helix in relation to its surroundings, thereby increasing the rate at which the protein folds and determining the pathway which is followed during folding (Sternberg *et al.,* 2000). These interactions are shown in Figure 1.5.

1.4.3 Dimer formation

Human GSTP1-1, unlike other GSTs, shows a level of cooperativity between its subunits under certain conditions (Ricci *et al.,* 1995; Bello *et al.,* 1998). The enzyme has hydrophobic associations that are required for the formation of the lock-and-key motif (Figure 1.6) which is found at the dimer interface, stabilising the individual subunits (Reinemer *et al.,* 1992). The key residue in the motif is Tyr50 which is inserted in a lock which is created by five amino acid residues (Met89, Gly93, Pro126, Phe127 and Leu130) that are situated in domain II of the second subunit (Ji *et al*., 1997). Upon substrate binding, Tyr50 becomes involved in 15 different interactions with the opposite subunit of the homodimer, while the same subunit in the apo form of the enzyme is only involved in only eight interactions (Oakley *et al*., 1998).

There are currently two main contrasting views concerning the existence of a stable monomer of GSTP1-1. Some studies have shown that unfolding of the enzyme leads to the formation of a structured monomer which is stable but inactive, and that the formation of the dimer is essential for the catalytic activity of the enzyme, (Aceto *et al.,* 1992). Other studies conducted by Dirr and Reinemer (1991) also showed that only the native, dimeric enzyme is active, but the monomer was found to be unstable. Any changes in the activity of the enzyme are therefore indicative of the disappearance or appearance of this species. Similar experiments conducted using hGSTP1-1 have shown that there is no stable monomer, but that the enzyme unfolds via

a dimeric intermediate which is inactive and has an extremely mobile α2-helix which is unfolded (Gildenhuys *et al.*, 2010).

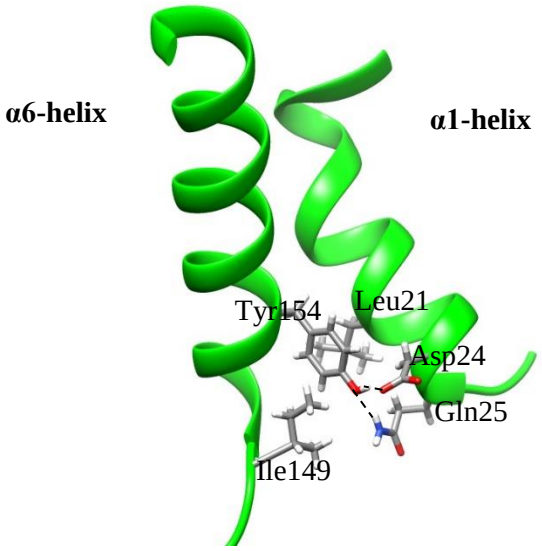

Figure 1.5: The hydrophobic staple motif which is found in human GSTP1-1 (PDB: 1GSY). The motif is represented by Ile149 in the N' position and Tyr154 inside the α6-helix occupying the N4 position. Tyr154 forms hydrogen bonds with Asp24 and Gln25, and hydrophobic interactions with Leu21 in the α1-helix. There is also a hydrophobic interaction between the side chain of Ile149 and the side chain of Tyr 154. UCSF Chimera (Pettersen *et al.*, 2004) was used to create the image of the crystal structure.

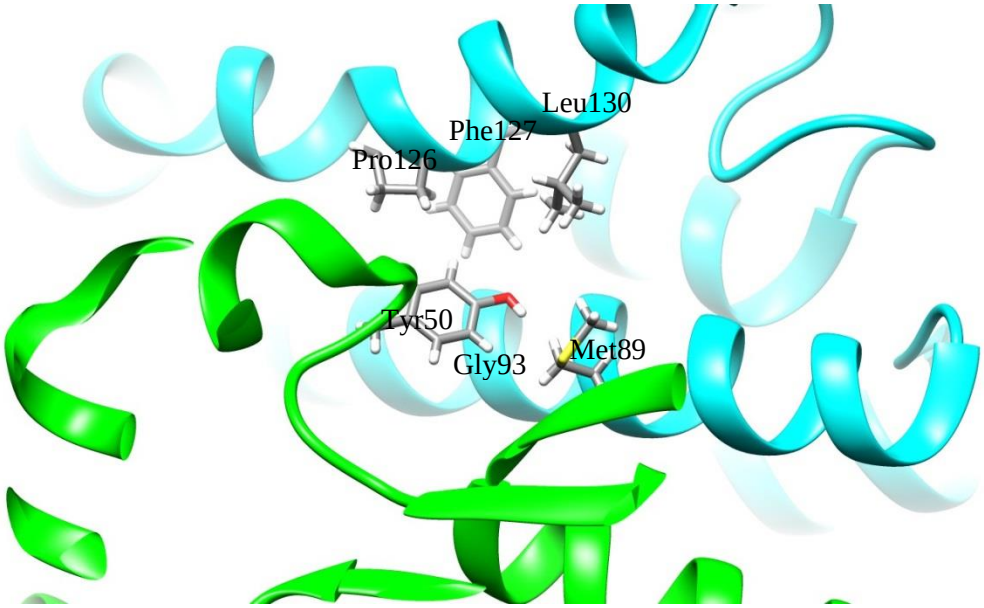

Figure 1.6: The lock and key motif at the dimer interface of hGSTP1-1. Tyr50 in one subunit (green) is the key residue which is wedged in a lock formed by Met89**,** Gly93, Pro126, Phe127 and Leu130 in the other subunit (cyan). Hydrophobic interactions between the residues are responsible for stabilising the individual subunits**.** UCSF Chimera (Pettersen *et al*., 2004) was used to create the image of the crystal structure.

1.4.4 Substrate binding

Human GSTP1-1 has a loop between the α2-helix and the β3-strand in a flexible region of the protein that contributes to one side of the G-site (Oakley *et al.*, 1998). As already described in section 1.4.3, substrate binding generally enhances the stability of the protein and the flexible region becomes less mobile to keep the substrate in place (Reinemer *et al*., 1992). Other studies have also shown that GSH binding protects GSTP1-1 from proteolysis by chymotrypsin (Lobello *et al.*, 1993). The cleavage site (Tyr44) becomes less exposed upon the binding of GSH, thus protecting it from proteolytic cleavage.

1.4.5 *S*-Nitrosation

S-Nitrosation is a post-translational modification of protein molecules that occurs when a covalent bond is formed between NO and the thiol of cysteine residues (Simon *et al*., 1996). Studies have shown that *S*-nitrosation at Cys47 of GSTP1-1 by GSNO occurs spontaneously when α2 is in an open conformation (Balchin *et al*., 2013). This results in a reduction in the activity of the enzyme by as much as 94% since this modification substantially increases the dynamics of the active site (Balchin *et al*., 2013). *S*-Nitrosation at Cys101 significantly destabilises domain 1 of GSTP1-1, which creates a somewhat disordered structure that unfolds with very low thermodynamic and kinetic cooperativity (Balchin *et al*., 2013). It also results in a refolding fault in domain 1, hindering the complete reconstruction of the native state of the protein. As well as destabilising domain 1, it has also been observed that *S*-nitrosation enhances the structural flexibility of certain regions of domain 2 (Balchin *et al*., 2013).

1.5 Non-classical roles of GSTP1-1

GSTP1-1 has other non-classical roles in addition to its main function as a detoxification enzyme. The enzyme also contributes to the development of drug resistance (Tew *et al.*, 1996), the regulation of the MAP kinase pathway (Adler *et al.* 1999), protecting cells from nitrosative stress by liberating NO while catalysing the degradation of nitro-compounds (Klatt *et al.*, 1999) and regulating the function of 1-Cys peroxiredoxin (Manevich *et al.*, 2004).

A high proportion of cancer cell lines from humans, including those that are resistant against anti-cancer drugs, express enhanced amounts of GSTP1-1 in comparison to the neighboring tissue (Mannervik *et al.*, 1987; Shea *et al.*, 1988). Inhibition studies have shown that the down-regulation of GSTP1-1 in T-cells favours apoptosis (Bernardini *et al*, 2000) and inhibition of the function of the enzyme induces apoptosis in rat hepatoma cells (Asakura *et al*., 2001). It

has also been shown that GSTP1-1 is the predominant isozyme in 97% of tumour cell lines that are used in drug screening programs. There is a significant quantitative correlation between the total enzyme, the enzymatic activity and mRNA, most notably in cell lines that are resistant to alkylating agents such as cyclophosphamide, cisplatin, BCNU (*N,N′*-bis(2-chloroethyl)-*N*-nitrosourea), chlorambucil, and melphalan (Tew *et al.*, 1996). As a consequence, GSTP1-1 expression is normally used as a reliable marker for cancer development, progression and drug resistance in patients that are recipients of chemotherapy (Tidefelt *et al.*, 1992; Howells *et al.*, 2004). The expression of GSTP1-1 in breast cancer was analysed by immunohistochemistry using the polyclonal anti-GSTP1-1 antibody and then compared with levels of the anti-apoptotic protein Bcl-2 (Huang *et al.*, 2003). Since enhanced levels of GSTP1-1 are found in cancer cells, certain drugs are designed in a manner that enables the enzyme to be involved in their metabolism in order to obtain the highest possible therapeutic index. Chemotherapeutic drugs such as TLK286 are administered as prodrugs and are designed in such a way that they undergo proton abstraction at the active site of GSTP1-1 which initiates a cleavage reaction, resulting in conversion of the inactive prodrug into cytotoxic products (Lyttle *et al*., 1994).

JNK is a mitogen-activated protein kinase (MAPK) that is involved in stress response (Rosette and Karin, 1996), inflammation (Ip and Davis, 1998), apoptosis, cellular differentiation and proliferation (Chen *et al.*, 1996). Protein synthesis inhibitors, ultraviolet (UV) radiation and other stress stimuli can activate JNK (Leppa and Bohmann, 1999), causing it to phosphorylate c-Jun, which is a constituent of a transcription factor known as activator protein-1 (AP-1) (Karin, 1995). The activation results in target genes that are dependent on AP-1 and are involved in cell death and cell proliferation being induced. GSTP1-1 associates with the c-Jun-JNK complex and prevents c-Jun from being phosphorylated by JNK (Adler *et al.* 1999). Most chemotherapeutic agents promote apoptosis through the activation of the MAPK pathways. The function that is played by GSTP1-1 as an inhibitor of JNK activation is directly linked to many drug-resistant tumours overexpressing the enzyme (Yin *et al.*, 2000). When GSTP1-1 expression is enhanced during chemotherapy, this changes the balance of codification of signalling pathways that control apoptosis and the proliferation of cells.

Nitric oxide (NO) is an important secondary messenger that is synthesised by nitric oxide synthases (NOS; Stuehr, 1997) and controls cellular signalling events (Isenberg *et al.*, 2009). The interaction of NO with glutathione, superoxide, oxygen or certain metals can result in *S*-glutathionylation of proteins, which is a post-translational modification that is extremely important to signalling pathways (West *et al*,. 2006). GSTP1-1 protects the cell from nitrosative

stress by liberating NO while also catalysing the breakdown of various nitro-compounds (Klatt *et al.*, 1999; Townsend *et al.*, 2006). Conversely, nitro compounds can directly alter the function of GSTP1-1 by lowering its affinity to GSH after the nitrosylation of Cys47 by *S*-nitrosoglutathione (Boese, *et al*., 1997).

1-Cys peroxiredoxin (1-CysPrx, Prdx6) is an antioxidant enzyme which is expressed in the cells of all major organs and has both acidic calcium-independent/lysosomal phospholipase A2 (aiPLA2, LPLA2) and GSH-peroxidase (Prx) activities (Manevich *et al.,* 2002; Wilson *et al.,* 2009). Studies have shown that GSTP1-1 is always needed for the function of 1-Cys Prx since it reactivates a Cys residue on Prx via GSH dependent reduction (Manevich *et al.,* 2004). It has also been shown that there is competition between JNK and 1-CysPrx for binding to GSTP1-1 and the two proteins consequently affect the activation of each other (Kim *et al.,* 2006).

As already highlighted, GSTP1-1 is responsible for protecting cells from damage by foreign chemicals and is also involved in many other roles. The enzyme is expressed in many human tissues, particularly in the renal distal convoluted tubules and the biliary tree (Terrier *et al*., 1990). Since GSTP1-1 has such a wide array of functions in human cells compared to other GST classes, it is important to thoroughly understand the general characteristics of the enzyme in terms of its structure, function and stability. This information would be useful in future studies since it would make it easier to design inhibitors of the protein and come up with strategies to manipulate how the protein functions inside target cells.

AIM AND OBJECTIVES

Aim

The aim of this study was to characterise the structure, function and stability of human glutathione *S*-transferase Pi using molecular biology and biophysical techniques.

Objectives

The objectives that had to be completed in this study to achieve the aim were seven-fold:

1. Express wild type human GSTP1-1 in *Escherichia coli* and purify the protein.
2. Characterise the secondary structure of hGSTP1-1 using far-UV circular dichroism.
3. Characterise the tertiary structure of hGSTP1-1 using intrinsic (Trp) fluorescence studies.
4. Characterise the quaternary structure of hGSTP1-1 using size exclusion HPLC.
5. Determine the non-catalytic ligandin function of the enzyme using ANS-binding studies and the catalytic function using a GSH-CDNB conjugation assay.
6. Determine the recovery of hGSTP1-1 after denaturation in 8 M urea.
7. Conduct stability studies on the enzyme using thermal melting and urea denaturation.

CHAPTER 2
EXPERIMENTAL PROCEDURES

2.1 Materials

The pET-15b vector encoding recombinant hGSTP1-1 was a generous donation from S.Y. Blond (Centre for Pharmaceutical Biotechnology, University of Illinois, Chicago) and T7 Express Competent Cells were purchased from BioLabs Inc. (Massachusetts, USA). Sequencing of the target insert encoding hGSTP1-1 was conducted by Inqaba Biotechnical Industries (Pty) Ltd (Pretoria, South Africa) using T7 promoter and T7 terminator primers. Carbenicillin was purchased from Roche Diagnostics (Basel, Switzerland). The HisTrap High Performance columns for protein purification were bought from Merck (Darmstadt, Germany). The reduced glutathione (GSH), 8-anilino-1-naphthalenesulfonic acid (ANS), urea and 1-chloro-2,4-dinitrobenzene (CDNB) were of ultrapure grade and were purchased from Merck (Darmstadt, Germany). Dithiothreitol was purchased from Inqaba Biotechnical Industries (Pty) Ltd (Pretoria, South Africa). All other chemical reagents that were used in this study were of analytical grade. All buffer solutions were prepared using milliQ water and had their pH confirmed using a Metrohm pH meter (Herisau, Switzerland). Data fitting was done using SigmaPlot version 14.0.0 (Systat Software Inc., California, USA).

2.2 Experimental procedures

2.2.1 Heterologous expression of hGSTP1-1

Transformation of T7 Express competent *Escherichia coli* cells was done using pET-15b plasmids encoding wild type hGSTP1-1 in terms of the protocol described by Chung *et al* (1989). The sequence landmarks of the pET-15b vector (Figure 2.1) include a T7 promoter that is 16 base pairs long to facilitate the strong binding of transcription factors, an ampicillin resistance selection marker, a histidine-tag coding sequence and a T7 terminator flanking the multiple cloning site. A representation of a pET-15b vector is shown in Figure 2.1. Single colonies were cultured overnight in 2×YT media (1% (w/v) yeast extract, 1.6% (w/v) tryptone and 0.5% (w/v) NaCl) supplemented with 50 µg/ml of carbenicillin at 37 °C and shaking at 230 rpm. The overnight cultures were diluted 1:50 using fresh 2×YT media supplemented with 50 µg/ml of carbenicillin and incubated at 37 °C and 230 rpm until the OD_{600} was approximately 0.5. The cultures were induced with isopropyl β-D-1-thiogalactopyranoside (IPTG) to a final concentration of 0.2 mM and cultured for additional 6 hours at 37 °C and 230 rpm.

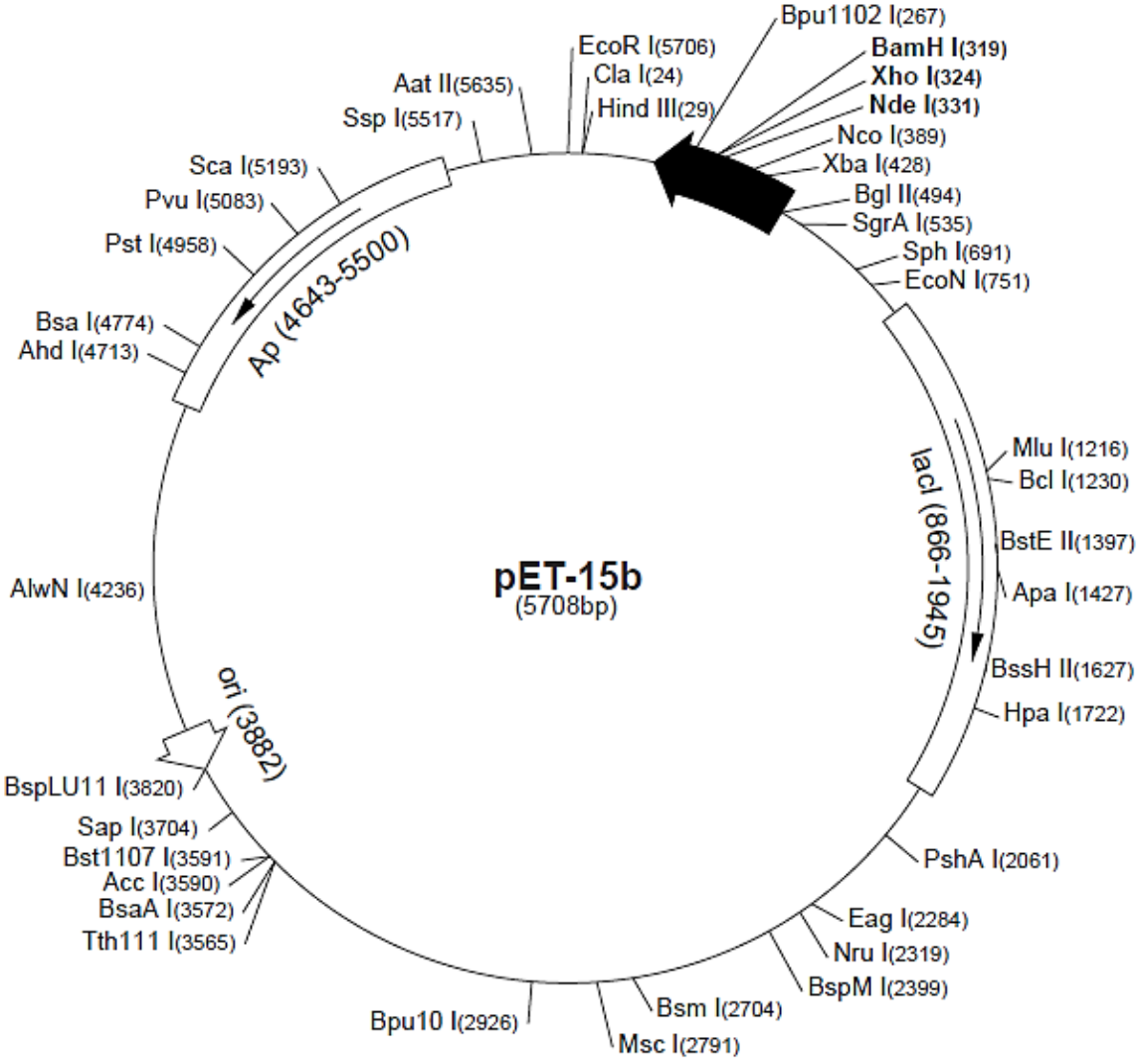

Figure 2.1: The plasmid map of a pET-15b vector. The major sequence landmarks include a T7 promoter (453-469), T7 transcription start site (452), a histidine-tag coding sequence (362-380), multiple cloning sites (*Nde*I - *Bam*H I) (319-335), a T7 terminator (213-259), a lacI coding sequence (866-1945), a pBR322 origin (388) and a *bla* coding sequence (4643-5500). The histidine-tag coding sequence is located between the *Nco* I and *Nde* I restriction sites. (Adapted from https://www.addgene.org/vector-database/2543/)

T7 Express cells have the T7 RNA polymerase gene which is inserted into the lac operon on the chromosome of *E.coli* and becomes expressed upon the addition of IPTG, leading to T7 promoter driven expression of hGSTP1-1. Cells were harvested after protein expression by centrifugation (6000×*g*, 4 °C, 15 minutes). Approximately 12.5 g of wet cell pellet was obtained from one litre of culture and the pellet was resuspended in 30 ml of 50 mM Tris-HCl, pH 8, 500 mM NaCl, 50 mM imidazole and 0.02% (w/v) NaN_3 (buffer 1) and then frozen at -80 °C overnight. The cell suspension that had been frozen was allowed to thaw at room temperature and disrupted using sonication on ice before centrifugation at 25000×*g* and 4 °C to obtain the soluble cell fraction.

2.2.2 Protein purification

The soluble cell fraction was subjected to immobilised metal affinity chromatography (IMAC; Porath and Olin, 1983) using an immobilised Ni^{2+} chelate resin (HisTrap HP column) connected to an ÄKTA FPLC protein purification system. The column (5 ml) was pre-equilibrated with 10 column volumes of buffer 1. The IMAC resin was subsequently washed using at least ten column volumes of buffer 1 in order to remove unbound or loosely-bound protein before eluting the bound protein from the column by a continuous gradient using 50 mM Tris-HCl, pH 8, 500 mM NaCl, 300 mM imidazole and 0.02% (w/v) NaN_3 (buffer 2). Fractions collected during the purification process were analysed by sodium dodecyl sulfate polyacrylamide gel electrophoresis (SDS-PAGE) (Laemmli, 1970) using a 4% stacking gel and a 12% resolving gel. Fractions containing the eluted protein were pooled and dialysed for 16 hours at 4 °C (with 2 changes of the buffer) against 20 mM sodium phosphate buffer, pH 7.4, with 0.02% NaN_3 and 2 mM dithiothreitol (DTT) (buffer 3). The quantity of the purified protein was ascertained using the theoretical extinction coefficient of hGSTP1-1 (55320 $M^{-1}cm^{-1}$) obtained using ProtParam (Gasteiger et al, 2005).

2.3 Structural characterisation

2.3.1 Secondary structure characterisation by far-UV circular dichroism

Circular dichroism is a spectroscopic technique that is used for measuring the absorption of right and left circularly polarised light (Greenfield and Fasman, 1969). Far-UV circular dichroism (CD) (180-250 nm) is sensitive to the conformation of the peptide backbone of a protein and therefore gives an indication of the secondary structure composition of the protein. Far-UV CD measurements of 4 µM hGSTP1-1 suspended in 5 mM sodium phosphate buffer, pH 7.4, with 0.02% (w/v) NaN_3 were done in a Jasco J-810 Spectropolarimeter at 20 °C. The

data was collected using a bandwidth of 1 nm, a scanning speed of 200 nm/min and 5 accumulations. The CONTINLL algorithm in the Dichroweb online server was used to evaluate the secondary structure of hGSTP1-1 by estimating the content of secondary structural elements using the circular dichroism data (Whitmore and Wallace, 2004). The server does this by determining the proportion of amino acid residues that are involved in the formation of α-helices, β-turns and β-sheets, in relation to the fraction of residues that are involved in random coils (Sreerama and Woody, 2000).

2.3.2 Tertiary structure characterisation by intrinsic fluorescence studies

Tryptophan, which usually occurs in one or a few residues in most protein molecules, was used as an intrinsic fluorescent probe. The fluorescence of the indole chromophore of tryptophan is extremely sensitive to the environment, making it ideal for reporting the tertiary structure of the protein and interactions with other molecules (Szabo and Rayner, 1980). Fluorescence spectra were obtained in triplicate using a Jasco FP 6300 spectrofluorometer (scan speed, 200 nm/min; excitation and emission band widths, 5 nm; data pitch, 1 nm; path length, 1 cm; excitation wavelength, 295 nm; 3 accumulations) at 20 °C. All spectral measurements were done in 5 mM sodium phosphate buffer, pH 7.4, with 0.02% (w/v) NaN_3 using 2 µM hGSTP1-1.

2.3.3 Quaternary structure characterisation by SE-HPLC

Size-exclusion high-performance liquid chromatography (SE-HPLC) is an analytic technique that separates molecules according to their molecular weight (Porath and Flodin, 1959). The molecular weight of hGSTP1-1 after purification by IMAC was determined at 20 °C by SE-HPLC using a TSKgel® SuperSW2000 HPLC column (4.6 × 300 mm) connected to an SW-type HPLC guard column. The buffer solution (20 mM sodium phosphate, pH 7.4, with 0.5 M NaCl and 0.02% (w/v) NaN_3) was degassed and filtered using a 0.45 µM filter prior equilibration of the column using a flow rate of 0.2 ml/min. The gel-filtration column was calibrated using BioRad gel filtration standards consisting of thyroglobulin (670 kDa), γ-globulin (158 kDa), ovalbumin (44 kDa), myoglobin (17 kDa) and vitamin B_{12} (1.4 kDa). The molecular weight of hGSTP1-1 was determined using 20 µl of protein.

2.4 Functional characterisation

2.4.1 GSH-CDNB conjugation assay

The catalytic activity of hGSTP1-1 was determined using the conjugation of reduced glutathione (GSH) to 1-chloro-2,4-dinitrobenzene (CDNB). The reaction was monitored spectrophotometrically at 340 nm as a result of the production of 1-(*S*-glutathionyl)-2,4-dinitrobenzene which has a molar absorption coefficient of 9600 $M^{-1}cm^{-1}$. The concentration of GSH was first confirmed using 5,5'-dithio-bis-(2-nitrobenzoic acid) (DTNB) which binds to the free sulfhydryl groups to produce a mixed disulfide and 2-nitro-5-thiobenzoic acid prior to performing the assay. The standard 3 ml assay volume contained 1 mM GSH, 1 mM CDNB and 3% (v/v) ethanol in 100 mM sodium phosphate buffer, pH 6.5 with 1 mM EDTA. Protein concentrations ranging from 6 nM to 28 nM were used. The assay was conducted at a pH of 6.5 because at this pH the rate of the non-catalysed reaction between GSH and CDNB is minimal. Conjugation reactions were carried out at 20 °C for 60 seconds, producing linear progress curves. The non-enzymatic control was subtracted from the enzymatic reactions before calculating the specific activity of the enzyme.

2.4.2 ANS-binding studies

The fluorescent probe 8-anilino-1-naphthalenesulfonic acid (ANS; Robinson *et al.,* 1978) was used to characterise hydrophobic regions on the structure of hGSTP1-1. All measurements were carried out in 5 mM sodium phosphate buffer, pH 6.5 using 200 µM of ANS and 2 µM hGSTP1-1. The four reactions (the buffer, 2 µM enzyme suspended in buffer, 200 µM ANS suspended in buffer and the combination of ANS plus enzyme suspended in buffer) were incubated at room temperature for an hour to allow sufficient binding of ANS to the protein. Fluorescence spectra were obtained in triplicate with a Jasco FP 6300 spectrofluorometer by exciting all the samples at 390 nm and monitoring the emission of light between 400 and 600 nm. The spectra were normalised by subtracting the spectrum of the buffer from the spectra of the free ANS, the enzyme only and the ANS plus enzyme. A spectrum of ANS bound to hGSTP1-1 was obtained by subtracting the emission spectrum of free ANS from the emission spectrum of ANS incubated with hGSTP1-1.

2.5 Stability studies

2.5.1 Thermal unfolding

Thermal unfolding is generally used to determine the stability of protein molecules (Privalov, 1979). Thermal-induced protein unfolding studies were done to assess the stability of hGSTP1-1 by monitoring changes in the α-helical content of the protein in response to changes in temperature. A solution of hGSTP1-1 was heated and subsequently cooled at a constant rate of 1 ºC.min^{-1} in the range between 20 ºC and 80 ºC using a Jasco PTC-423S Peltier type temperature control system attached to a water cooling bath. Perturbations in the secondary structure of the protein were monitored using far-UV circular dichroism in a Jasco J-810 spectropolarimeter (band width, 1 nm; path length, 2 mm; response time, 0.5 s; data pitch, 0.1 ºC) by monitoring changes in the ellipticity at 222 nm. Unfolding was done using 2 µM protein in 5 mM sodium phosphate buffer, pH 7.4, with 0.02% (w/v) NaN_3. The mean residue ellipticity (in deg.cm^2.dmol^{-1}`) was calculated from the ellipticity using the equation:

$$[\theta] = \frac{\theta \times 100}{l \times N \times c} \quad (1)$$

where θ is ellipticity in millidegrees, l is the path length in cm, N is the number of amino acid residues in hGSTP1-1 and c is the protein concentration in mM.

2.5.2 Urea-induced unfolding studies

2.5.2.1 Recovery of denatured hGSTP1-1

In order to assess the conformational stability of hGSTP1-1, the amount of recovered protein after denaturation in 8 M urea and subsequent refolding was determined. A 9.5 M stock solution of ultra-pure urea was prepared and the concentration was confirmed using an ATAGO pocket refractometer. The control reaction was prepared by suspending 2 µM protein in 1.6 M urea and incubating the solution for 1 hour at room temperature. The experimental reaction was prepared by suspending 10 µM protein in 8 M urea, incubating the solution for an hour at room temperature before preparing a 5 times dilution of the protein solution using the buffer in order to obtain a final protein concentration of 2 µM. The diluted solution was incubated for another hour at room temperature to allow for sufficient refolding of the protein. All solutions and dilutions were prepared using 5 mM sodium phosphate buffer, at pH 6.5, with 0.02% (w/v) NaN_3. A concentration of 1.6 M urea was chosen for this study since this concentration is found in the pre-transition region of the unfolding curve of hGSTP1-1. A comparison of the protein

concentration in the 2 samples was made using the UV-Visible spectra of hGSTP1-1 in the control and experimental reactions between 240 nm and 340 nm. Differences in the tertiary structure of hGSTP1-1 in the control and experimental samples were analysed by comparing Trp fluorescence emission spectra obtained using a Jasco FP-6300 spectrofluorometer (scan speed, 200 nm/min; with excitation and emission band widths of 5 nm; data pitch, 1 nm; path length, 1 cm; excitation wavelength, 295 nm; 3 accumulations) at 20 °C.

2.5.2.2 Urea-induced equilibrium unfolding

The unfolding transition of hGSTP1-1 was determined using urea as a denaturant to ascertain how stable the protein is. Urea-induced unfolding of 2 µM hGSTP1-1 was conducted in 5 mM sodium phosphate buffer, pH 6.5 over a range of urea concentrations between 0 M and 8 M. All samples were first incubated at room temperature to allow for equilibrium to be reached before analysis by far-UV circular dichroism (section 2.3.1) and fluorescence spectroscopy (section 2.3.2). Far-UV CD was used to monitor changes in the ellipticity at 222 nm, which is indicative of changes in the secondary structure of hGSTP1-1 when the protein becomes denatured. Fluorescence was used to monitor changes in the fluorescence spectra of tryptophan residues in hGSTP1-1 since the environment of these residues changes as the protein becomes unfolded.

The equilibrium unfolding data that were obtained were analysed according to a two-state unfolding pathway of a dimeric protein. When a dimeric protein unfolds reversibly following a two-state model, a point of equilibrium is reached between the native (N) and unfolded (U) species:

$$N_2 \leftrightarrow 2U \tag{2}$$

It should also be noted that during a two-state unfolding transition, it is exclusively the native and unfolded states of the protein that are present at noteworthy concentrations (Pace, 1986). Hence, for a two-state unfolding mechanism:

$$f_N + f_U = 1 \tag{3}$$

where f_N represents the proportion of native protein and f_U represents the proportion of unfolded protein. The fraction of unfolded protein was then determined using the equation:

$$f_u = \frac{(y_N - y_0)}{(y_N - y_U)} \tag{4}$$

where y_0 is the circular dichroism signal, f_N represents the fraction of unfolded protein, and f_U represents the fraction of unfolded protein. Furthermore, y_N represents the y value for the folded state (extrapolated from the pre-transition region of the unfolding curve), while y_U represents the y value for the unfolded state (extrapolated from the post-transition region of the unfolding curve). The equilibrium constant (K_{eq}) between the native and unfolded states at a given concentration of urea was calculated using the equation:

$$K_{eq} = \frac{f_U}{1-f_U} \quad (5)$$

The values of K_{eq} that were obtained were used to calculate the free energy change of unfolding ($\Delta G°$) using the standard relationship:

$$\Delta G° = -RT\ln K_{eq} \quad (6)$$

where R is the gas constant (8.314 $J.K^{-1}.mol^{-1}$) and T is the absolute temperature. In order to determine $\Delta G_{(H2O)}$ it is assumed that $\Delta G°$ has a linear dependence on denaturant concentration for all concentrations of urea, according to the linear free-energy model (Tanford, 1968). Therefore:

$$\Delta G° = \Delta G_{H20} + m[\text{urea}] \quad (7)$$

where $\Delta G_{(H2O)}$ represents the free energy difference between the native and unfolded states when there is no urea, m is the m-value for the dependence of free energy on the concentration of urea which is also an indicator of cooperativity, and [urea] is the molar concentration of urea.

The CD equilibrium unfolding data that were obtained were fitted using SigmaPlot version 14.0.0. according to the standard equation:

$$f = F_U(y_u - y_n) + y_n \quad (8)$$

CHAPTER 3
RESULTS

3.1 Plasmid verification

A portion of the four-colour chromatogram that was obtained from Chromas™ for the sequencing analysis done by Inqaba Biotec is shown in Figure 3.1. The DNA sequence has Quality (Q) values ranging from 31 to 58 and even distances between the individual peaks. Q values are obtained by taking the $\log_{10}$ of the error probability and multiplying it by -10. This means that the nucleotide bases have error probabilities ranging between 1 in 1259 to 1 in 630957. All the peaks in Figure 3.1A are well-defined and have minimal background-noise. There are no missing (N) nucleotides in the data or any heterozygous (double) peaks.

The results obtained from the Basic Local Alignment Search Tool (BLASTx) (Figure 3.1B) show that the query sequence obtained from Inqaba biotec was a perfect match (100% identity) with the sequence of human glutathione *S*-transferase Pi (GSTP1-1) (sequence identity: NP_000843.1) in the protein database. The match had an E-value of 3×10^{-146}, which is a measure of the expected number of chance alignments (Altschul *et al*., 1990). The sequence was reliable and there is a very low probability that the match between the query sequence and hGSTP1-1 was as a result of a chance alignment.

3.2 Overexpression of hGSTP1-1

The successful recombinant overexpression of hGSTP1-1 in *Escherichia coli* was achieved using 0.2 mM isopropyl β-D-1-thiogalactopyranoside as an inducer at 37 ºC and shaking at 230 rpm for 6 hours. A 12% (w/v) SDS-PAGE resolving gel that was used to analyse the products of the overexpression alongside a control sample is shown in Figure 3.2A. The gel shows the Precision Plus Protein Dual Xtra Standards in lane 1. There are no pronounced GST protein bands in both the soluble and insoluble fraction of the control sample (0 mM IPTG) in lanes 2 and 3. However, there is a thick GST protein band in the soluble fraction of the sample that was induced with 0.2 mM IPTG in lane 5. The linear plot that was used to determine the approximate size of the overexpressed protein is shown in Figure 3.2B. The highlighted protein band in lane 5 has a molecular mass of approximately 23 kDa, which corresponds to the mass of a single subunit of hGSTP1-1 (Mannervik, 1985).

.

A

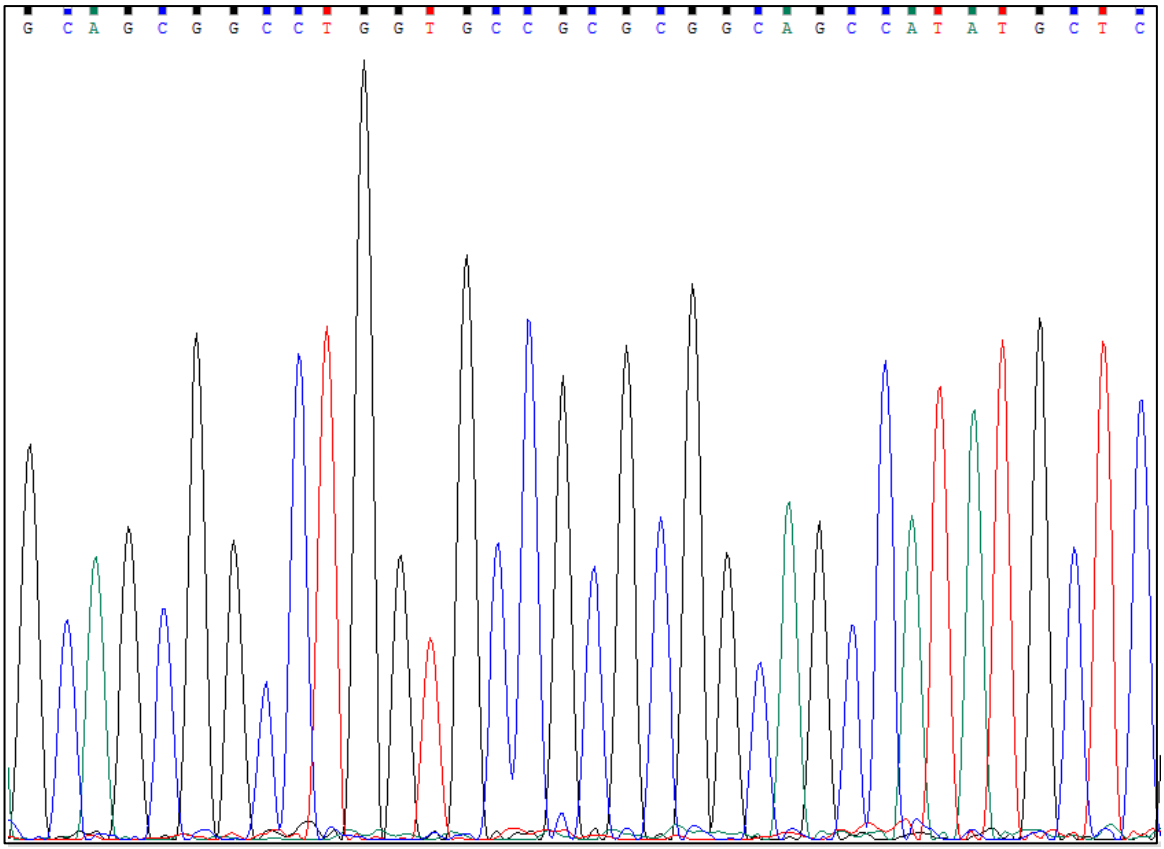

B

Score	Expect	Method	Identities	Positives	Gaps	Frame
416 bits(1069)	3e-146	Compositional matrix adjust.	203/203(100%)	203/203(100%)	0/203(0%)	+2

```
Query  101  PPYTVVYFPVRGRCAALRMLLADQGQSWKEEVVTVETWQEGSLKASCLYGQLPKFQDGDL  280
            PPYTVVYFPVRGRCAALRMLLADQGQSWKEEVVTVETWQEGSLKASCLYGQLPKFQDGDL
Sbjct  2    PPYTVVYFPVRGRCAALRMLLADQGQSWKEEVVTVETWQEGSLKASCLYGQLPKFQDGDL  61

Query  281  TLYQSNTILRHLGRTLGLYGKDQQEAALVDMVNDGVEDLRCKYISLIYTNYEAGKDDYVK  460
            TLYQSNTILRHLGRTLGLYGKDQQEAALVDMVNDGVEDLRCKYISLIYTNYEAGKDDYVK
Sbjct  62   TLYQSNTILRHLGRTLGLYGKDQQEAALVDMVNDGVEDLRCKYISLIYTNYEAGKDDYVK  121

Query  461  ALPGQLKPFETLLSQNQGGKTFIVGDQISFADYNLLDLLLIHEVLAPGCLDAFPLLSAYV  640
            ALPGQLKPFETLLSQNQGGKTFIVGDQISFADYNLLDLLLIHEVLAPGCLDAFPLLSAYV
Sbjct  122  ALPGQLKPFETLLSQNQGGKTFIVGDQISFADYNLLDLLLIHEVLAPGCLDAFPLLSAYV  181

Query  641  GRLSARPKLKAFLASPEYVNLPI  709
            GRLSARPKLKAFLASPEYVNLPI
Sbjct  182  GRLSARPKLKAFLASPEYVNLPI  204
```

Figure 3.1: Sequencing of the cloned hGSTP1-1 expression cassette in the pET-15b vector. Sequencing of the pET-15b vector was done using T7 primers**.** Panel A shows a portion of the chromatogram obtained during sequencing by Inqaba biotec. The DNA sequence has Quality values ranging from 31 to 37 and even distances between the individual peaks. The chromatogram has very little background noise. Panel B shows results of the alignment that was done using BLASTx. The query sequence was 100% identical to the sequence of glutathione *S*-transferase Pi (polymorphism A).

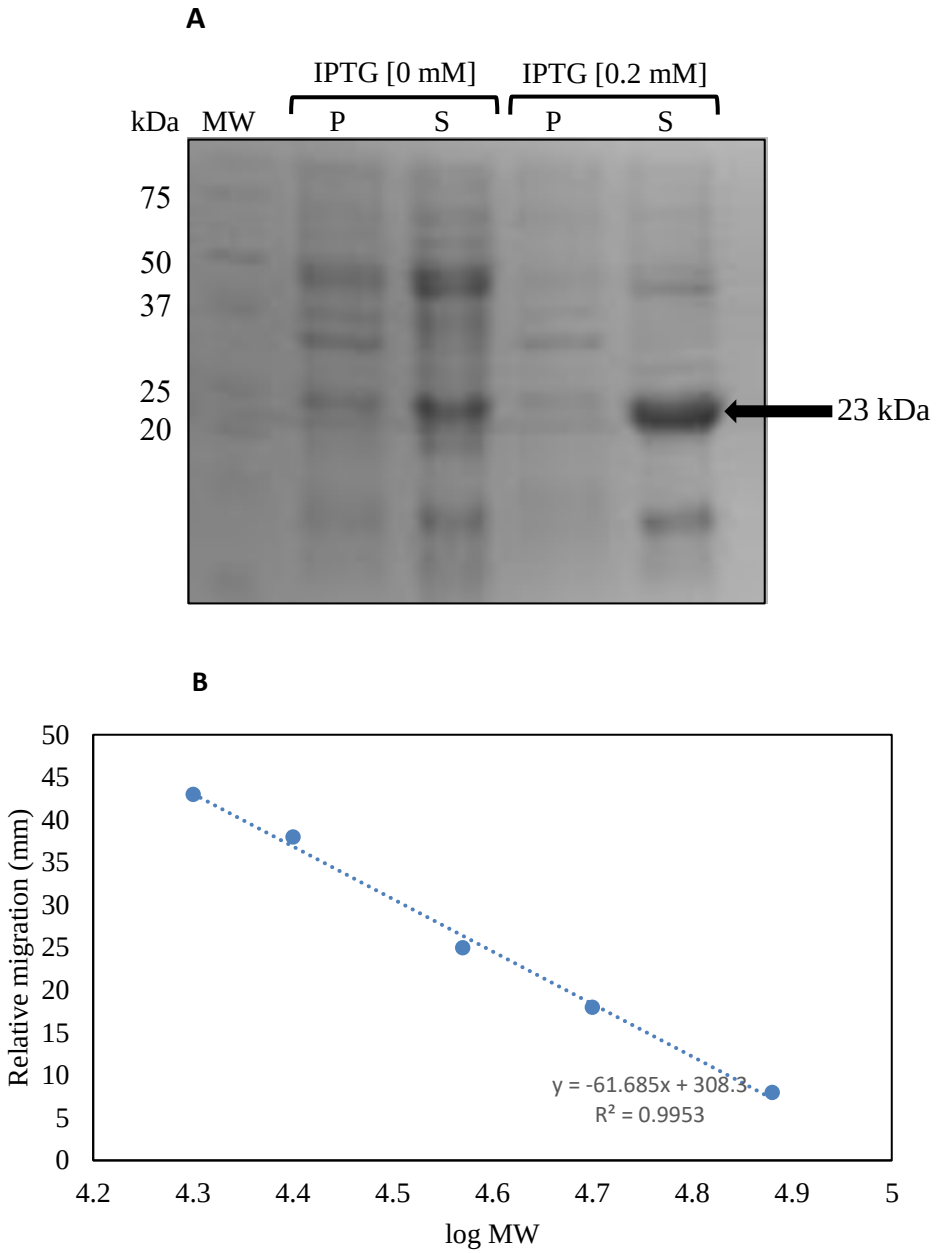

Figure 3.2: A 12% resolving SDS-PAGE gel that was used to analyse the overexpression of hGSTP1-1. Induction of heterologous protein expression was done in *Escherichia coli* cells using 0.2 mM IPTG at 37 ºC and 230 rpm for 6 hours. The samples that were analysed in Panel **A** (from left to right) are Precision Plus Protein Dual Xtra Standards (MW), the insoluble fraction of the control (P), the soluble fraction of the control (S), the insoluble fraction of the induced cell culture (P) and the soluble fraction of the induced cell culture (S). Panel B shows the standard curve ($y = -61.685x + 308.3$ and R^2=0.9953) that was used to determine the molecular mass of the overexpressed protein. The highlighted protein has a mass of approximately 23 kDa when determined using the equation.

3.3.1 Purification of hGSTP1-1

The elution profile that was used to monitor the purification of hGSTP1-1 from the cell lysate using immobilised metal affinity chromatography (IMAC) is shown in Figure 3.3. Peak 1 represents the *E.coli* soluble fraction that did not bind to the immobilised Ni^{2+} ligand, while the protein that was tightly bound to the nickel ions is shown by peak 3. Peak 2 represents an unknown protein that was less tightly bound to the resin than the protein in peak 3 and therefore eluted from the IMAC column by 170 mM imidazole. The red line represents the concentration of imidazole that was used for binding protein molecules to the IMAC resin, washing of unbound molecules and elution of the bound protein from the column. The protein that had the highest affinity for the Ni^{2+} ions was eluted from the IMAC column using 200 mM imidazole.

3.3.2 Purity assessment

The samples that had been collected during protein purification were analysed by denaturing SDS-PAGE as shown in Figure 3.4. The 12% resolving gel shows that when the soluble cell fraction (S) was passed through the IMAC column, most of the overexpressed protein was bound to the resin, since the prominent band in lane 2 is not visible in lane 3. Peak 2 (Figure 3.3) does not represent the overexpressed protein, since the prominent band in lane 2 (Figure 3.4) is not present. The eluted protein in fraction 3 corresponds to the overexpressed protein (hGSTP1-1) observed in lane 2. According to the elution profile, the electrophoretogram and the linear plot, pure protein samples with a molecular mass of approximately 23 kDa were eluted from the Ni^{2+}-IMAC column using 200 mM imidazole.

UV-Visible spectroscopy was used to check if the protein sample obtained using IMAC had any nucleic acid contamination, since the technique detects non-protein contaminants between 240 nm and 340 nm. The spectrum that was obtained is shown in Figure 3.5. The combined fractions (3 in Figure 4) had an A_{280} of 2.09 and a 260/280 nm absorbance ratio of 0.51, which is indicative of a pure protein sample (Glasel, 1995). The peak in the absorbance reading at 280 nm is due to the presence of tryptophan and tyrosine residues in protein molecules (Glasel, 1995; Pace *et al*., 1995).

The concentration of pure protein was 5.5 mg/ml and there was a total of 66 mg of protein obtained from 1 litre of cell culture.

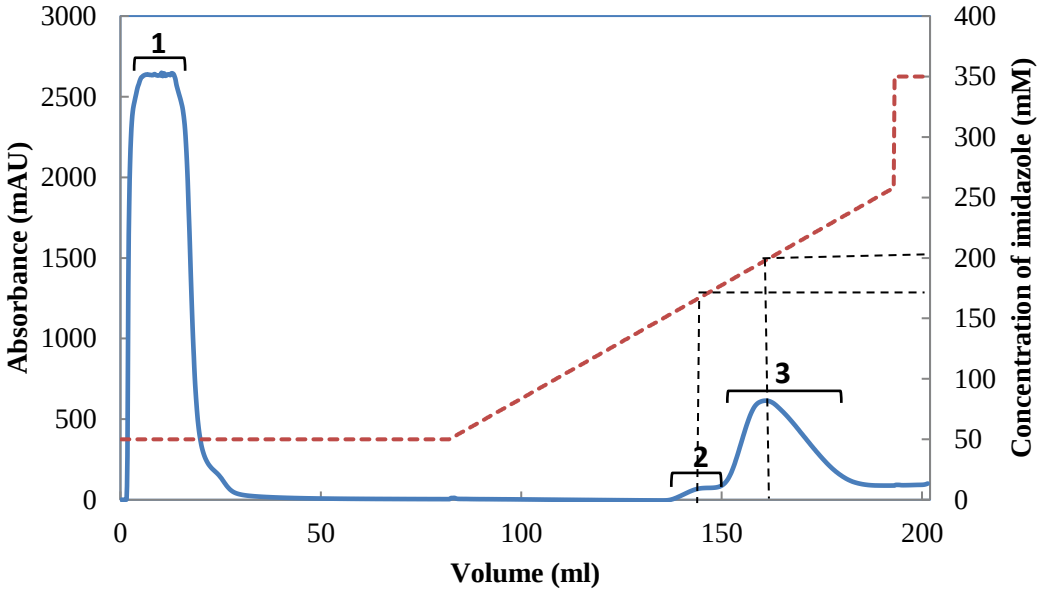

Figure 3.3: The elution profile for the purification of hGSTP1-1using Ni^{2+} immobilised metal affinity chromatography. Peak 1 represents the flow through, while peak 3 represents the protein that was bound to the IMAC column. Peak 2 represents an unknown protein that was bound less tightly to the IMAC column. The red broken line indicates the concentration of imidazole (in 50 mM Tris-HCl, pH 8, with 0.5 M NaCl and 0.02% (w/v) NaN_3) that was used during the binding, washing and elution steps of the purification process. The bound protein was eluted from the IMAC column using 200 mM imidazole.

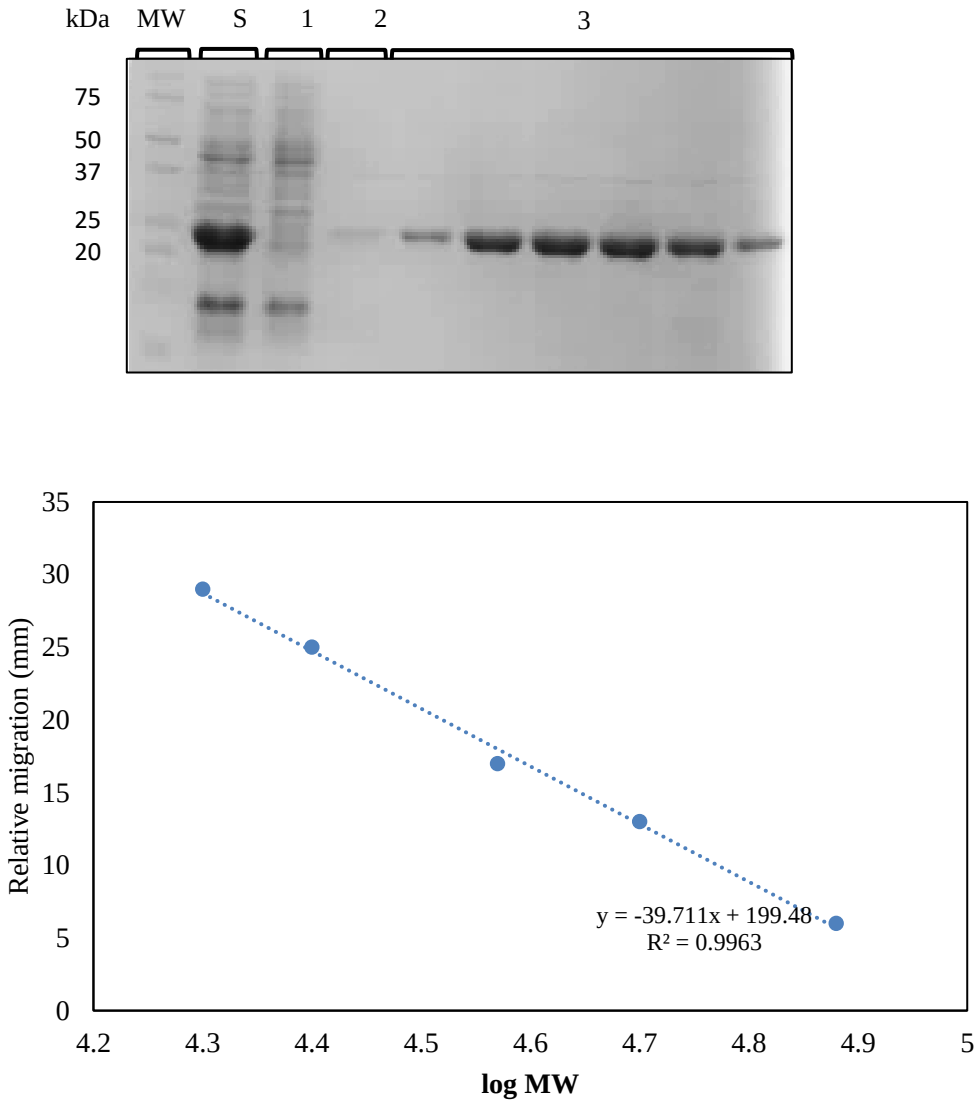

Figure 3.4: A 12% SDS-PAGE gel used for the analysis of samples collected during the purification of GSTP1-1. The samples from left to right are Precision Plus Protein Dual Xtra Standards (MW), the soluble fraction of the cell lysate (S), the flow through (1), the undefined sample (2) and the eluted protein that was bound to the Ni^{2+}-IMAC resin (3). According to the standard curve shown in panel B ($y = -39.711x + 199.48$ and R^2=0.9963), the eluted protein had a molecular mass of approximately 23 kDa.

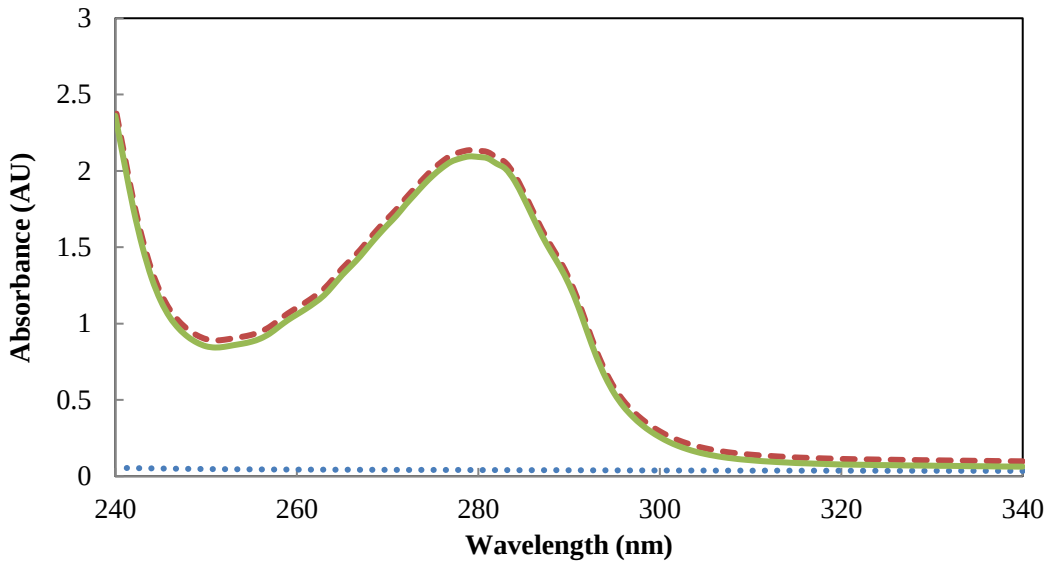

Figure 3.5: The UV-Visible spectrum of pure hGSTP1-1 between 240 nm and 340 nm. The corrected spectrum of the protein is shown in green, while the spectrum of the protein in the buffer is shown in red. hGSTP1-1 was in 20 mM sodium phosphate buffer, pH 7.4, with 0.02% (w/v) NaN_3. The spectrum of the buffer is shown in blue. Purified hGSTP1-1 had 260/280 nm absorbance ratio of 0.51.

3.4 Functional characterisation

3.4.1 GSH-CDNB conjugation assay

The specific activity of hGSTP1-1 was determined using a GSH-CDNB conjugation assay (Habig *et al*., 1974). Upon addition of 1 mM of the substrate (1-chloro-2,4-dinitrobenzene) there was a linear increase in the A_{340} reading. Figure 3.6 shows only one progress curve when 20 nM of hGSTP1-1 was used to catalyse the reaction. Representing the data in this way was done to avoid presenting an untidy graph with too many lines and equations. The progress curves for all the other concentrations are shown in the appendix (Figure A).The wavelength (340 nm) measures the amount of product (GS-DNB) in the solution (Mannervik and Danielson, 1988). The linear region on the progress curves indicates that the catalytic activity is dependent on the amount of enzyme present, which allows the specific activity to be calculated accurately using this assay (Watson *et al*., 1998). Table 3.1 shows a summary of the properties of the progress curves obtained for the conjugation assay. The gradient of each of the progress curves represents the initial velocity (v_0) of the conjugation reaction in the presence of the different concentrations of the enzyme. The enzyme activity (in μmol/min) was plotted against the amount of enzyme (in mg) (Figure 3.7). The specific activity (in μmol/min/mg) was obtained from the gradient of this plot. Human GSTP1-1 has a specific activity of 55.5 μmol/min/mg.

3.4.2 Extrinsic fluorescence: ANS-binding studies

Extrinsic fluorescence studies were done using 8-anilinonaphthalene-1-sulfonic acid (ANS) as a fluorescent probe. ANS has a low fluorescence signal in aqueous environments, but becomes highly fluorescent in non-polar, organic solvents or when it binds to solid phases (Weber and Laurence, 1954). The results obtained in this study show that the quantum yield of ANS increases significantly when it binds to hydrophobic regions on hGSTP1-1 (Figure 3.9). The binding of ANS to hGSTP1-1 results in a blue shift from 521 nm (free ANS) to 500 nm (ANS in the presence of protein) and nearly a two-fold increase in the fluorescence intensity (Figure 3.8). The figure also shows the spectrum of the bound ANS which was obtained by subtracting the spectrum of free ANS from the spectrum of ANS in the presence of protein.

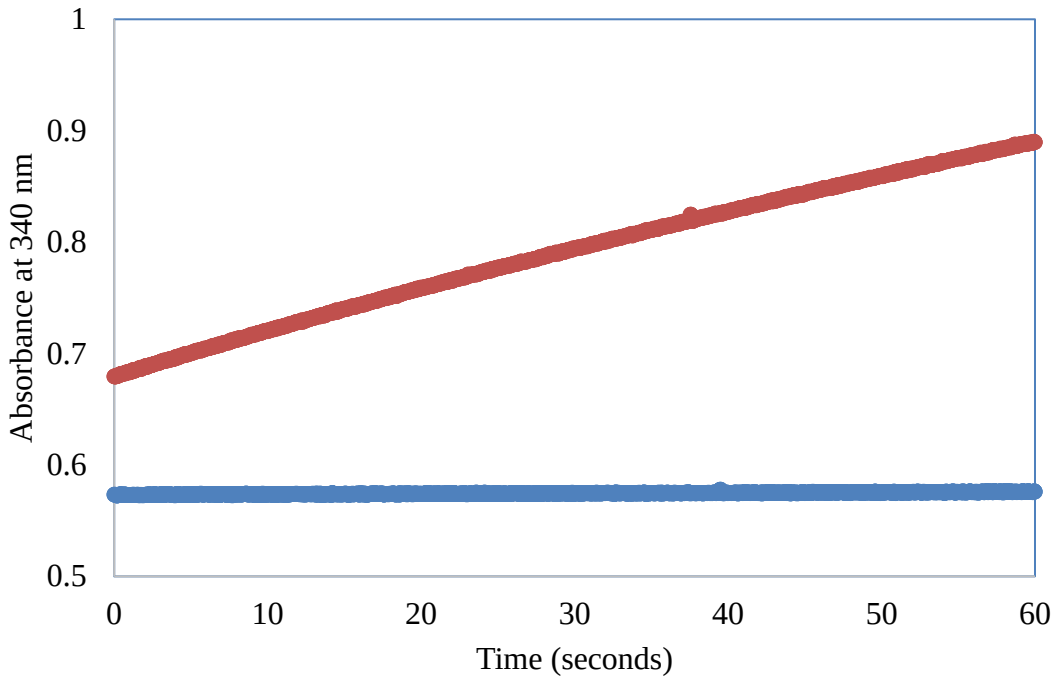

Figure 3.6: Absorbance at 340 nm plotted as a function of time to determine the catalytic activity of GSTP1-1. The CDNB-GSH conjugation assay was done by mixing 1 mM CDNB, 1 mM GSH and 20 nM protein at a pH of 6.5. The progress curve that is shown in red has not been corrected for the non-enzymatic control (blue).

Table 3.1: A summary of the properties of the progress curves obtained for a GSH-CDNB conjugation assay catalysed by hGSTP1-1. Absorbance at 340 nm was plotted as a function of time to determine the activity of the enzyme. The assay was done by mixing 1 mM CDNB, 1 mM GSH and increasing concentrations of protein at a pH of 6.5. All the values that are shown have been corrected for the non-enzymatic control (0 nM protein).

[hGSTP1-1] (nM)	Slope*	R^2 *
6	6×10^{-4}	0.998
8	14×10^{-4}	0.999
10	18×10^{-4}	0.999
12	21×10^{-4}	0.999
14	23×10^{-4}	0.999
16	26×10^{-4}	0.999
18	25×10^{-4}	0.999
20	34×10^{-4}	0.998
22	38×10^{-4}	0.998
24	40×10^{-4}	0.998
26	44×10^{-4}	0.997
28	48×10^{-4}	0.997

***The slopes were determined by linear regression of the progress curves. The R^2 values represent the linear fit to the progress curves.

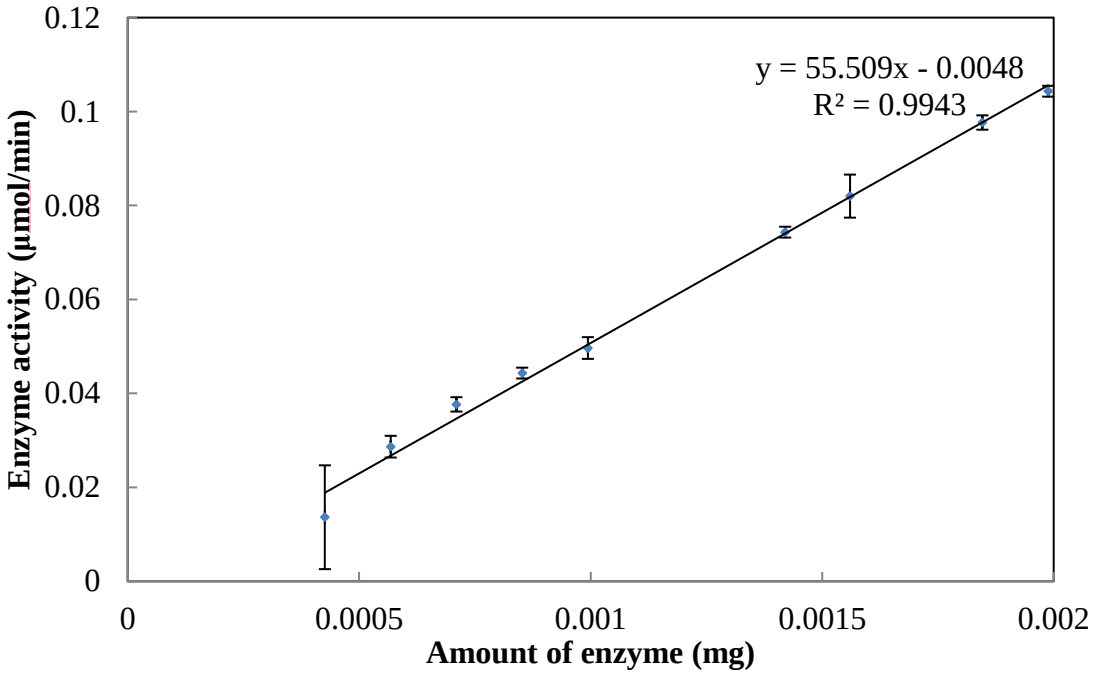

Figure 3.7: A plot of enzyme activity vs amount of enzyme used to determine the specific activity of GSTP1-1. The conjugation of reduced glutathione to 1-chloro-2,4-dinitrobenzene was monitored by monitoring the formation of the product (1-(*S*-glutathionyl)-2,4-dinitrobenzene) at 340 nm. The reaction was performed in triplicate in 0.1 M sodium phosphate buffer with 0.02% (w/v) NaN_3 and 1 mM GSH and 1 mM CDNB. The error bars represent the standard deviation of the replicates and the enzyme activity has been corrected for the non-enzymatic reaction. Human GSTP1-1 was calculated to have a specific activity of 55.5 µmol/min/mg as determined from the slope of the plot, which corresponds to published literature.

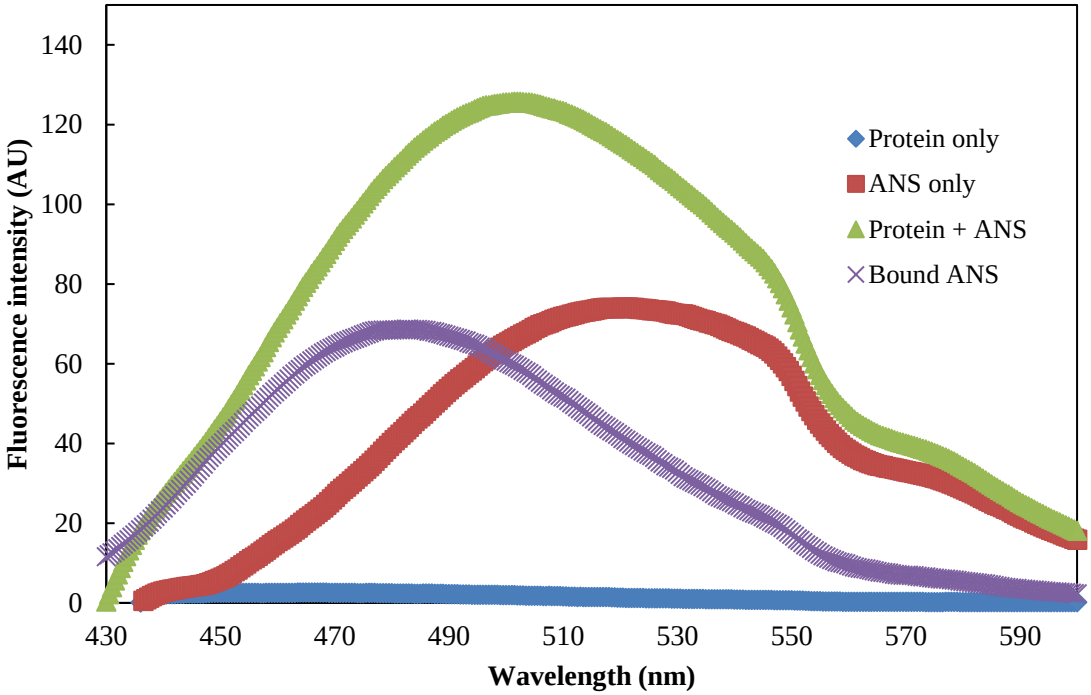

Figure 3.8: Extrinsic fluorescence studies done using 200 µM 8-anilinonaphthalene-1-sulfonic acid (ANS) as a fluorescent probe. The spectra of free ANS (red) and the spectra of ANS bound to hGSTP1-1 (green) are shown alongside the spectrum of bound ANS (purple). All samples were in 5 mM sodium phosphate buffer, pH 6.5 and the spectra were obtained at 20 °C. Binding of ANS to hGSTP1-1 results in a blue shift from 521 nm (free ANS) to 500 nm (ANS + protein) and a significant increase in the fluorescence intensity. The spectrum of bound ANS has a maximum emission wavelength at 483 nm.

3.5 Structural characterisation

3.5.1 Secondary structure characterisation by far-UV CD

Circular Dichroism (CD) in the far-UV range (190-250 nm) was used to study the secondary structure of hGSTP1-1 at 20 ºC. The CD spectrum that was obtained (Figure 3.9) has large negative values at 208 nm and 222 nm, which is indicative of a protein which is largely alpha-helical (Woody, 1995). The results that were obtained from the DICHROWEB server (Table 3.2) also confirm that the hGSTP1-1 is predominantly alpha-helical (Sreerama and Woody, 2000; Whitmore and Wallace, 2004). These results are consistent with crystallised structures of hGSTP1-1 which show that the protein has 54.5% of its amino acid sequence in alpha helices and only 8.6 % in beta sheets (Quesada-Soriano *et al*., 2009; Shishido *et al*., 2017).

3.6.2 Tertiary structure characterisation using intrinsic fluorescence studies

The tertiary structure of hGSTP1-1 was studied using tryptophan fluorescence. Although this technique is normally used to monitor changes in the tertiary structure of protein molecules, it can also be used to determine if a particular protein has tryptophan residues. The emission spectrum that was obtained after excitation at 295 nm (Figure 3.10) shows that the native protein has an emission maximum at 343 nm. This fluorescence signal is due to the presence of two tryptophan residues (Trp28 and Trp38) in each subunit of the dimer (Reinemer *et al*., 1992).

3.6.3 Quaternary structure characterisation

3.6.3.1 Size exclusion high performance liquid chromatography

Size-exclusion chromatography is a widely used technique for the determination of the quaternary structure of protein molecules. Figure 3.11A shows the chromatograms of hGSTP1-1 and the gel filtration standards that were obtained after analysis by SE-HPLC. The retention time that was observed does not correspond to either one of the two possible species of hGSTP1-1 (the folded dimer or the unfolded monomers). Instead, hGSTP1-1 had a retention time which corresponds to a folded monomer of the protein. According to the standard calibration curve that was used to determine the quaternary structure of native hGSTP1-1 (Figure 3.11B), the protein has a mass of 24 kDa.

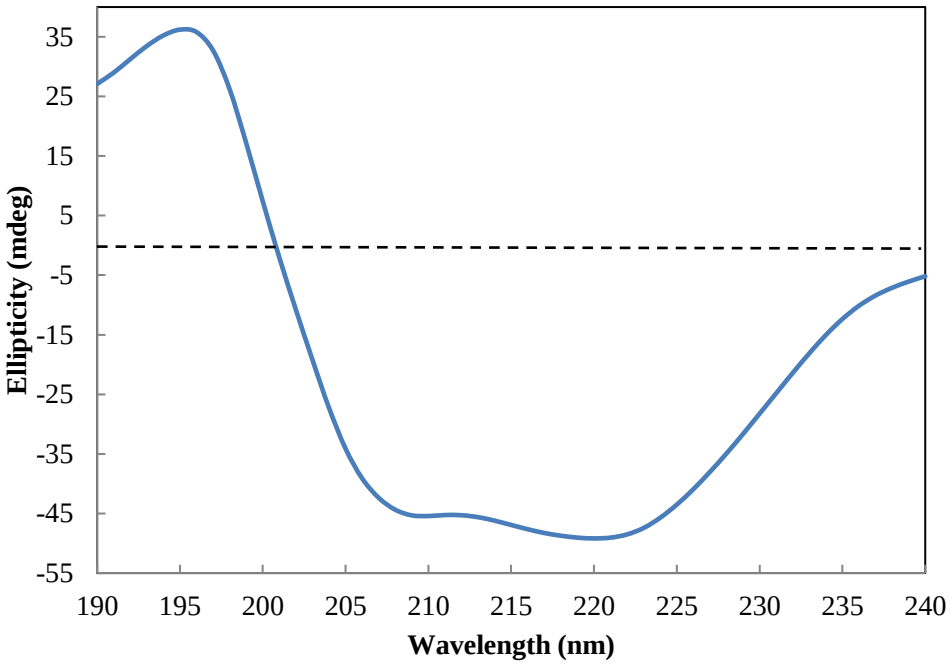

Figure 3.9: The far–UV circular dichroism spectrum of hGSTP1-1 monitored between 190-240 nm. The analysis was done at 20 ˚C in 5 mM sodium phosphate buffer, at pH 7.4, with 0.02 % (w/v) NaN_3. The spectrum has large negative values at 208 nm and 222 nm, which is indicative of a largely alpha-helical protein.

Table 3.2: The results that were obtained from the DICHROWEB server for the analysis of the secondary structure of hGSTP1-1. The fit had a normalised root mean square deviation of 0.183. The results show that only alpha helices were detected by the server (Whitmore and Wallace, 2008).

Parameter	Score (%)
Helix segments per 100 residues	22.908
Average helix length per segment	4.365
Strand segments per 100 residues	0.000
Average strand length per 100 residues	0.000

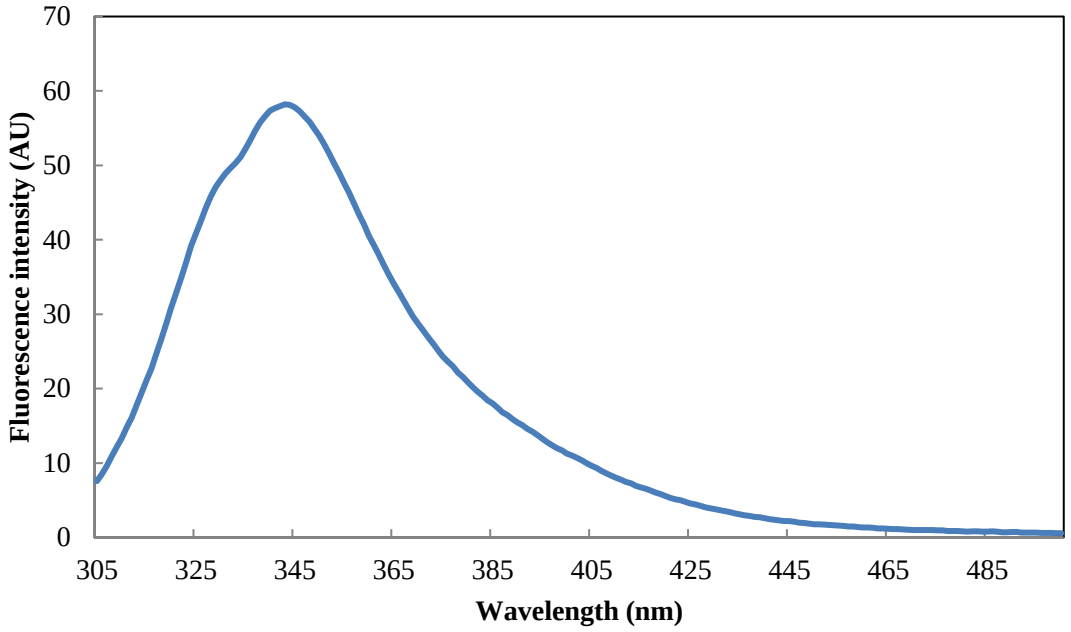

Figure 3.10: The tryptophan fluorescence emission spectrum of hGSTP1-1 after excitation at 295 nm. Analysis of the tertiary structure was done at 20 ˚C in 5 mM sodium phosphate buffer, at pH 7.4, with 0.02 % (w/v) NaN_3. Native hGSTP1-1 has an emission maximum at 343 nm.

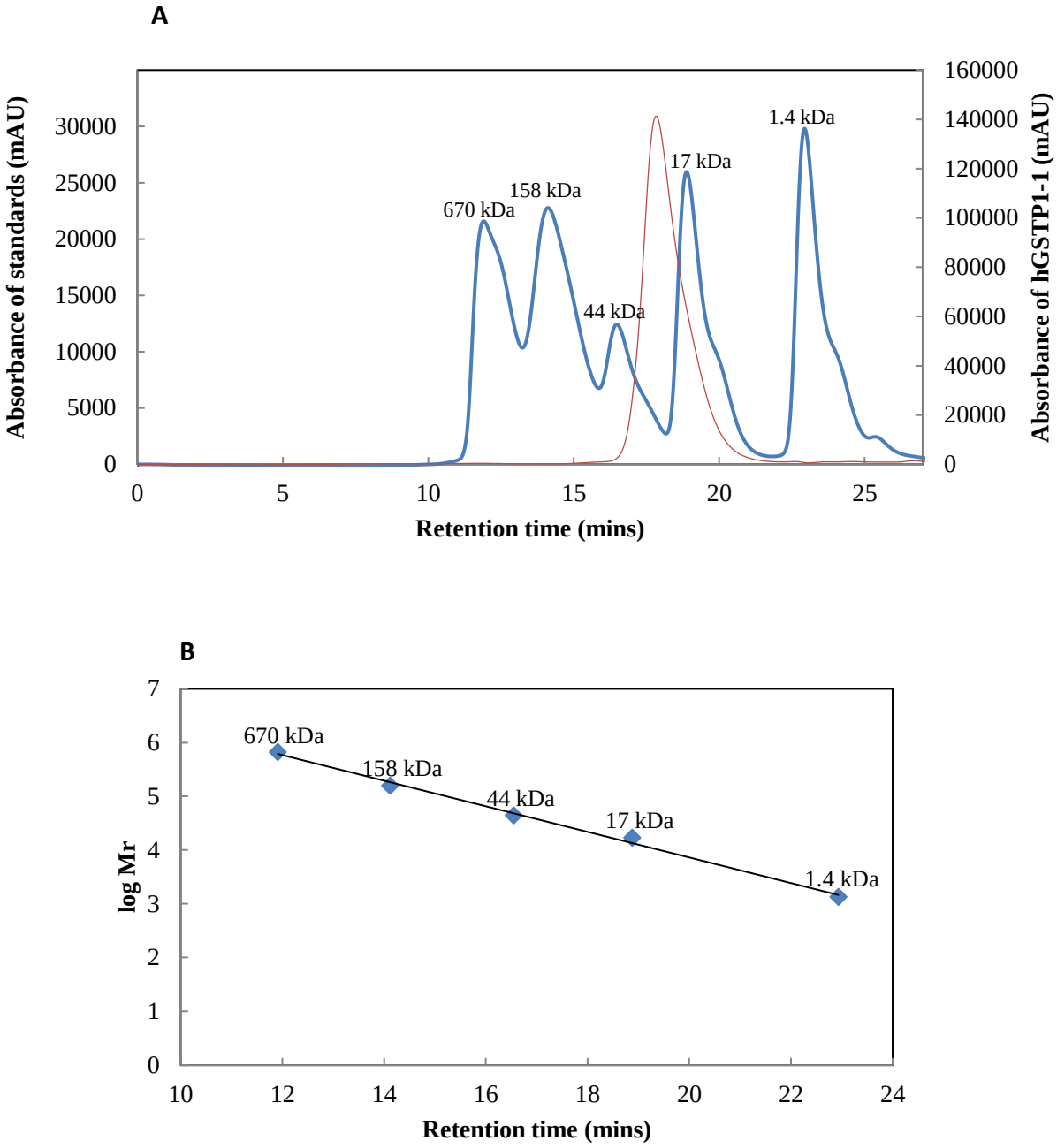

Figure 3.11: The chromatograms for BioRad gel filtration standards (blue) and hGSTP1-1 (red) when analysed by size exclusion HPLC. Panel A shows the chromatograms for the standards and hGSTP1-1. The standards that were used are thyroglobulin (670 kDa), γ-globulin (150 kDa), ovalbumin (44 kDa), myoglobin (17 kDa) and vitamin B_{12} (1.4 kDa). Panel B shows the calibration curve ($y = -0.2381x + 8.6245$ *and* $R^2 = 0.9955$) used to determine the molecular mass of native hGSTP1-1. The molecular mass of hGSTP1-1 is 24 kDa. Analysis was done using a SuperSW2000 HPLC column (4.6 × 300 mm) connected to an SW-type HPLC guard column.

3.6 Stability studies

3.6.1 Thermal-induced unfolding

The thermal unfolding of hGSTP1-1 was monitored using far-UV CD spectroscopy by heating the protein solution at a constant rate between 20 °C and 80 °C. Figure 3.12 shows the melting curve of hGSTP1-1. Refolding of the protein was attempted by cooling the sample of the unfolded protein at a constant rate from 80 °C to 20 °C. The pre-transition region is between 20-49 °C, the transition region is between 48-57 °C and the post-transition region is between 57-80 °C. However, hGSTP1-1 does not lose all of its secondary structure, because the mean residue ellipticity of the protein does not increase to 0 $deg.cm^2.dmol^{-1}$.

The refolding curve (also Figure 3.12) shows that the unfolding of hGSTP1-1 is irreversible, since there was no significant decrease in the ellipticity of the protein. This irreversibility would have resulted from the formation of aggregates as the protein became denatured. The aggregates were seen as a feint white suspension in the cuvette after the heating and cooling of the protein sample. Aggregates of protein molecules during unfolding made it impossible to analyse the transition using equilibrium thermodynamics (Benjwal *et al*., 2006).

3.6.2 Urea-induced unfolding

3.6.2.1 Recovery of denatured hGSTP1-1

The fluorescence spectrum of 2 μM hGSTP1-1 in 1.6 M urea (the control) was compared to the spectrum of 10 μM of the same protein which had been denatured using 8 M urea and then diluted 5-fold to 1.6 M urea using urea-free buffer. When refolding of hGSTP1-1 was done from its completely unfolded state in 8 M urea, there was limited recovery of the tryptophan fluorescence and λ_{max}. According to Figure 3.13, the recovered protein sample had a maximum fluorescence intensity of 573 AU, while the control sample had a maximum intensity of 484 AU. This means that only 84% of the denatured protein was recovered.

UV-Visible spectroscopy was used to compare the concentrations of hGSTP1-1 in the control and the recovered protein sample. Both samples had A_{280} values of 0.08. However, there were differences in the absorbance values at high wavelengths. This means that the differences obtained in the fluorescence intensities of the two samples may have been due to slight differences in the concentration of hGSTP1-1 in the control and experimental samples.

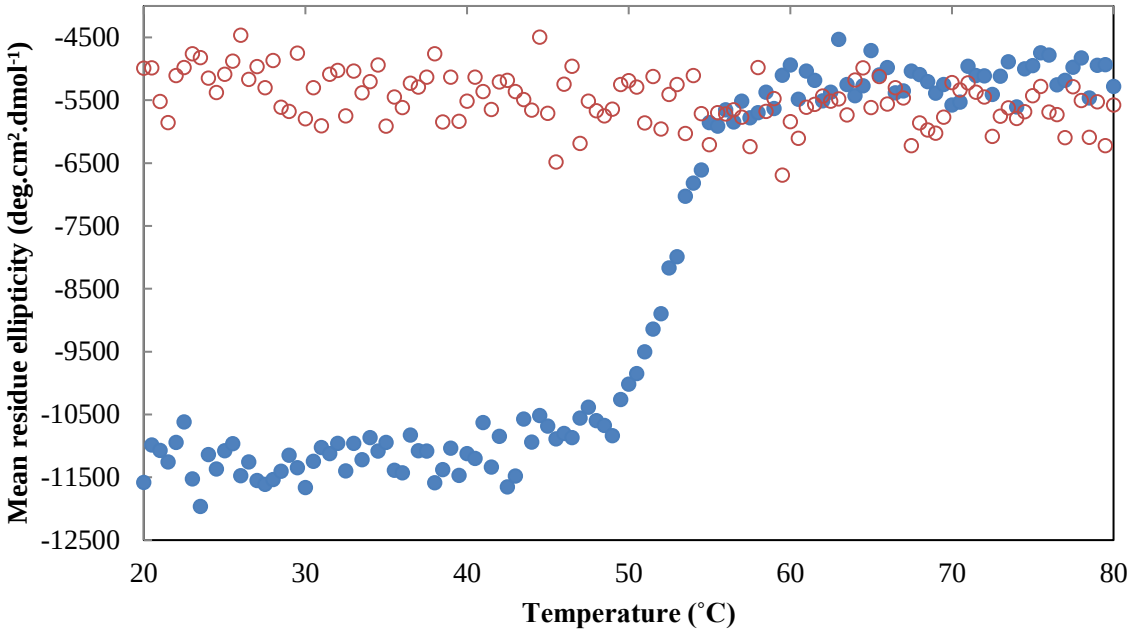

Figure 3.12: Thermal melting curve of hGSTP1-1 monitored between 20 °C and 80 °C. The pre-transition region is between 20-49 °C, the transition region is between 48-57 °C and the post-transition region is between 57-80 °C. Refolding of the denatured protein was attempted by lowering the temperature from 80 °C to 20 °C (red). There was no significant decrease in the mean residue ellipticity of the unfolded protein with a decrease in temperature.

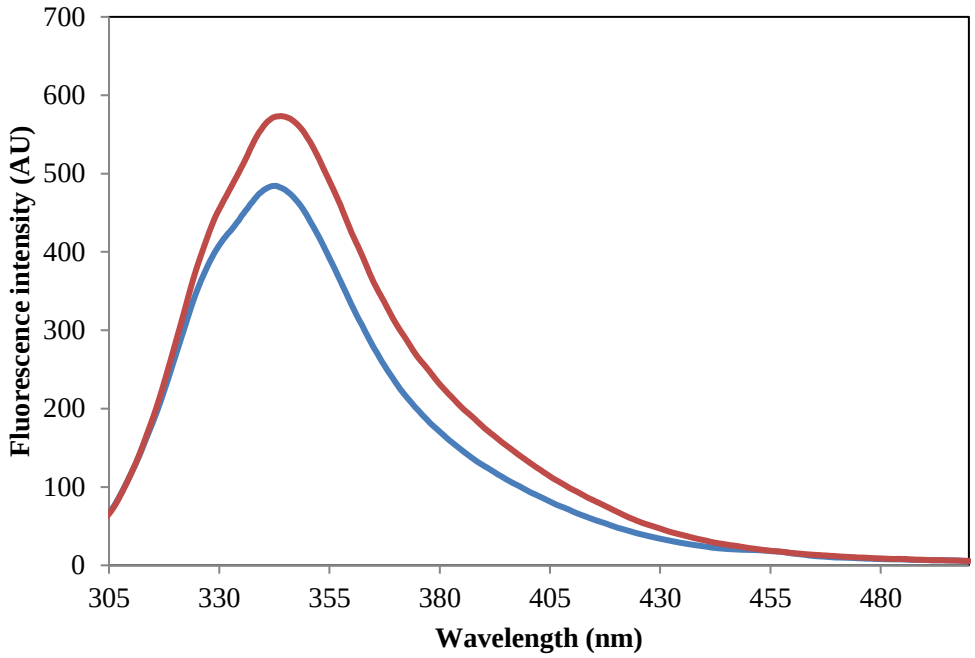

Figure 3.13: Fluorescence emission spectra of 2 µM of hGSTP1-1 used to assess the recovery of the denatured protein. Recovery was initiated from 8 M urea by a 5-fold dilution of the denatured protein using urea-free buffer. The spectra for the control sample are shown in blue, while the recovered protein is shown in red. Excitation of Trp residues was done at 295 nm and the emission was monitored between 250 nm and 500 nm. The maximum yield of the control is 484 AU and that of the recovered protein is 573 AU. This translates to 84% recovery of the denatured protein. All samples were in 5 mM sodium phosphate buffer, pH 6.5 with 1.6 M urea and analysed at 20 ˚C. Both samples had an A_{280} of 0.08 after the spectra were corrected for the blank.

3.6.2.2 Changes in the secondary structure of hGSTP1-1

Far-UV CD was used to monitor changes in the secondary structural content of hGSTP1-1 with an increase in the concentration of urea. Although a total of 41 urea concentrations were used to study the stability of the protein (Figure 3.15), only a few of them are shown in Figure 3.14 as they are the ones that have a bigger impact on the secondary structure of hGSTP1-1. Figure 3.14 shows that there was an increase in the ellipticity from -15.12 mdeg (in 0 M urea) to -2.76 mdeg (in 8 M urea). This indicates that there was a loss of alpha-helicity as the protein became denatured. The helical content in the protein decreases drastically between 4.6 M and 5 M urea. These concentrations are in the transition region of the unfolding curve of hGSTP1-1 (Figure 3.15)

The unfolding curve of hGSTP1-1 was plotted using the ellipticity at 222 nm for the protein in the presence of 0 M to 8 M urea (Figure 3.15), in 0.2 M increments. Changes in the ellipticity at 222 nm show that there is no formation of a partially unfolded stable intermediate state during the unfolding of the protein, since there is only a single transition. The pre-transition region of hGSTP1-1 is between 0-3.8 M urea, the transition region is between 3.8 M and 5.4 M and the post-transition region is between 5.4 M and 8 M. The transition midpoint is 4.6 M urea. The thermodynamic parameters for the two-state unfolding of hGSTP1-1 are shown in Table 3.3.

3.6.2.3 Changes in the tertiary structure of hGSTP1-1

Changes in the intrinsic Trp fluorescence are commonly used as a reliable probe to monitor any changes in the structure during the unfolding of protein molecules. Figure 3.16 shows the fluorescence emission spectra of hGSTP1-1 when the protein was exposed to increasing concentrations of urea (between 0 M and 8 M). The spectra that are shown in the figure correspond to the concentrations represented in Figure 3.14, since these are the concentrations that were expected to have the biggest influence on the tertiary structure of the protein. Unfolding of the protein results in a change in the emission maximum (λ_{max}) from 341 nm to 350 nm and an overall increase in the fluorescence intensity from 4.0 AU to 7.2 AU. There is, however, a decrease in the maximum fluorescence intensity between 4.2 M and 5.2 M urea. Figure 3.17 shows that the maximum emission of fluorescence increases substantially when the protein is exposed to increasing urea concentrations between 0 M and 4 M. The values then decrease between 4 M and 5.4 M urea, before increasing again between 5.4 M and 8 M urea.

The ratio of the fluorescence intensity for the unfolded protein (350 nm) to that of the folded protein (341 nm) after excitation at 295 nm when hGSTP1-1 was in the presence of increasing concentrations of urea was also used to monitor changes in the fluorescence of the protein. This ratio gives an indication of the stability of the regions of the protein molecule surrounding tryptophan residues. F_{350}/F_{341} begins to increase when the protein is in 2.8 M urea and becomes relatively constant between 6 M and 8 M urea as shown in Figure 3.18.

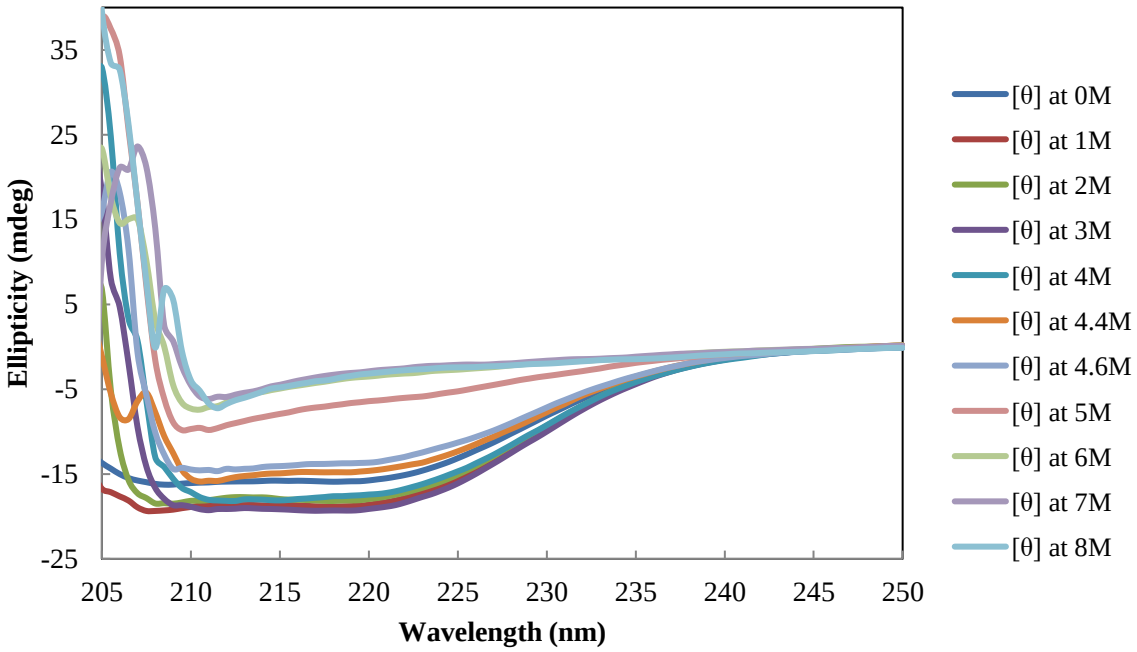

Figure 3.14: Far-UV CD spectra that were used to monitor changes in the secondary structure of hGSTP1-1 with an increase in the concentration of urea. There was an overall increase in the mean ellipticity at 222 nm from -15.12 mdeg (in 0 M urea) to -2.76 mdeg (in 8 M urea) at 20 ˚C. Unfolding was done in 5 mM sodium phosphate buffer, pH 6.5. The most drastic structural change in the secondary structure of the protein was observed between 4.6 M and 5 M urea.

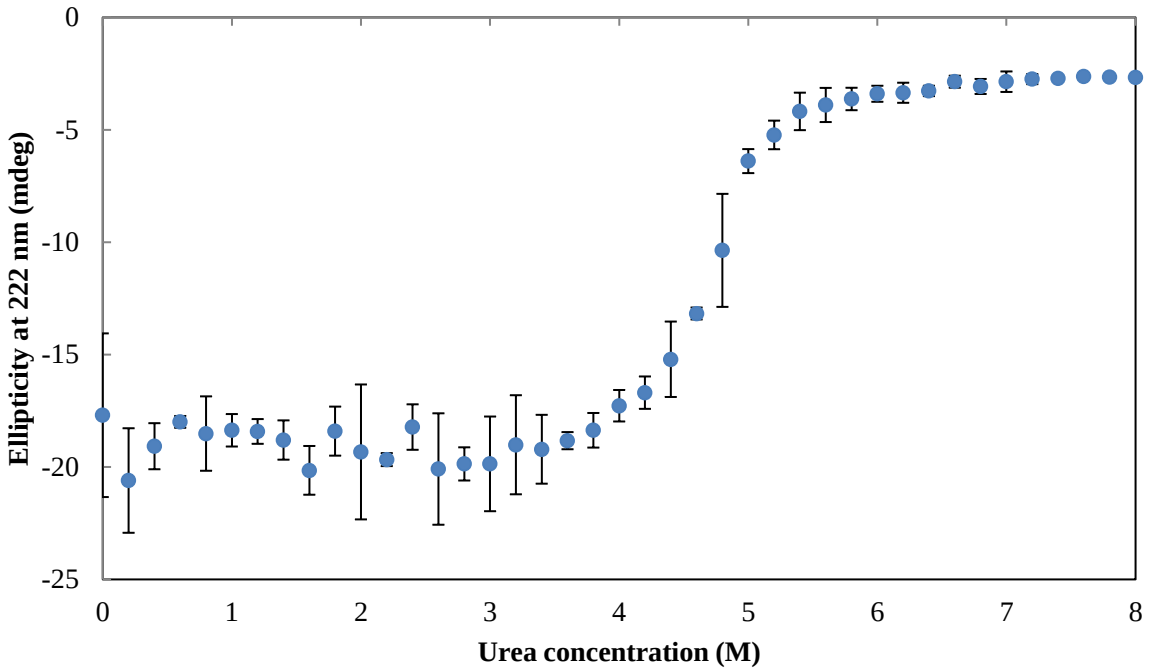

Figure 3.15: The urea-unfolding of hGSTP1-1 monitored by far-UV circular dichroism. Unfolding was monitored by plotting the ellipticity at 222 nm against the concentration of urea between 0 M and 8 M urea. The pre-transition region is between 0 M and 3.8 M urea, the transition region is between 3.8 M and 5.4 M urea and the post-transition region is between 5.4 M and 8 M urea. Denaturation on the protein was done at 20 °C in 5 mM sodium phosphate buffer, pH 6.5. The experiment was done in triplicate and the error bars represent the standard deviation of the replicates.

Table 3.3: Thermodynamic parameters of two-state equilibrium unfolding for hGSTP1-1. The values obtained are from fitting the equilibrium unfolding data to a two–state model for a dimeric protein. (N2 → 2U) using the equation $f = F_U(y_u - y_n) + y_n$ (see appendix for the parameters that were used).

	Far-UV CD	**Intrinsic fluorescence**
ΔG_{2HO} (kJ.mol^{-1})	5.3336	9.7424
C_m (molar urea)	4.6	4.2
***m*-value (kJ.mol^{-1}.molar urea)**	10.32	0.0125
R^2	0.9925	0.9031

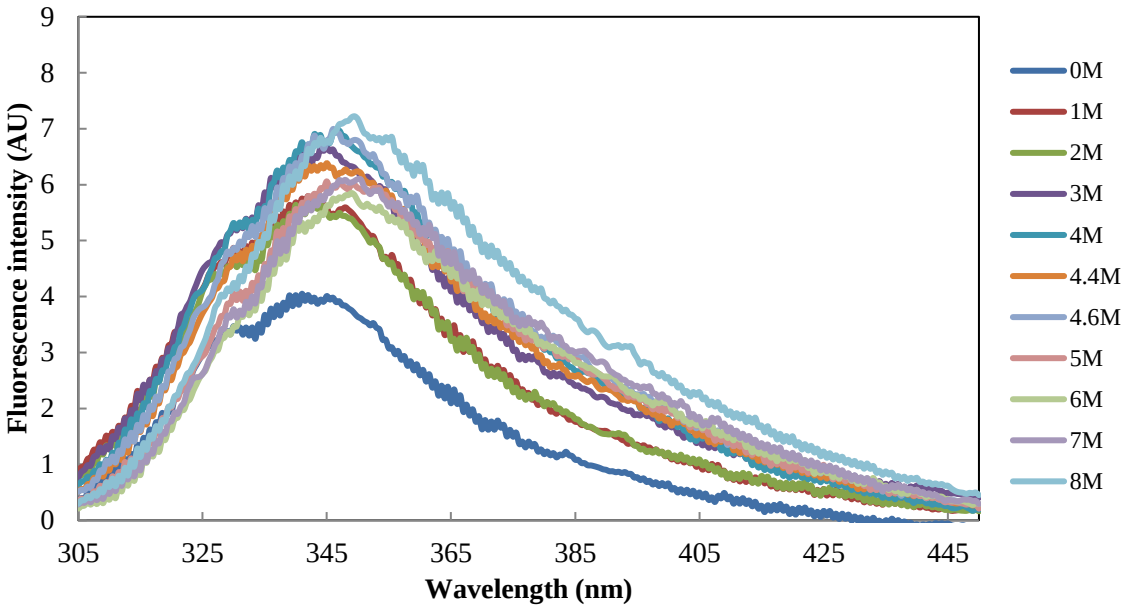

Figure 3.16: Fluorescence emission spectra of hGSTP1-1 when the protein was exposed to increasing concentrations of urea. Unfolding of the protein results in a red shift from 341 nm to 350 nm and an increase in the fluorescence intensity from 4.0 AU to 7.2 AU. All unfolding reactions were done in 5 mM sodium phosphate buffer, pH 6.5 at 20 ˚C and excitation of Trp residues was done at 295 nm.

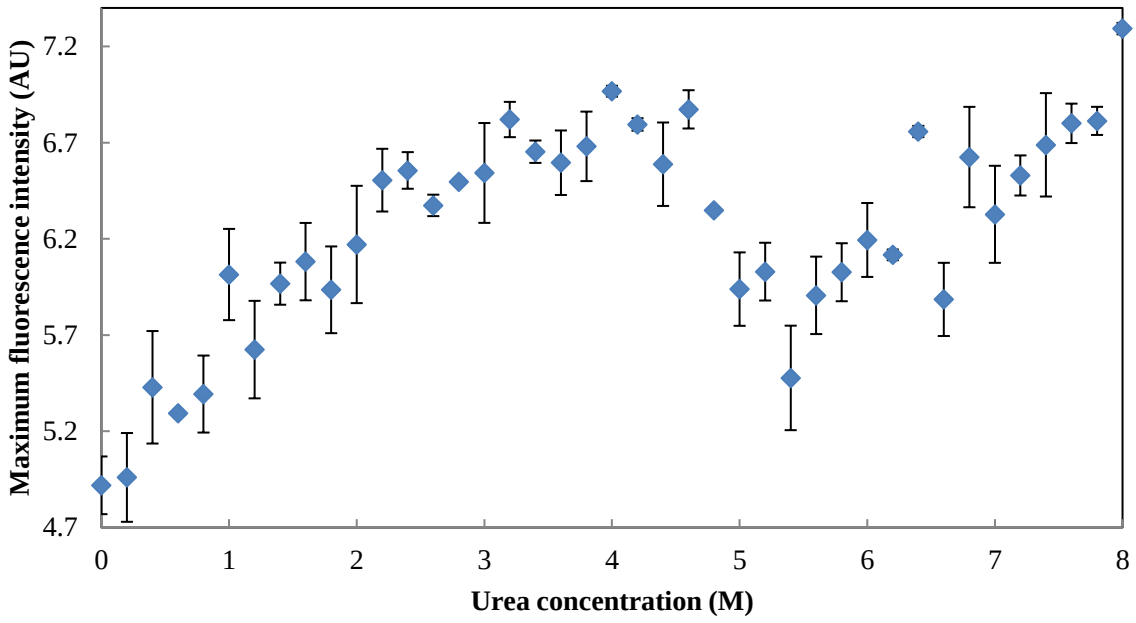

Figure 3.17: Changes in the maximum fluorescence of emission of hGSTP1-1 plotted as a function of the concentration of urea. Excitation of Trp residues was done at 295 nm and unfolding was done in 5 mM sodium phosphate buffer, pH 6.5 at 20 ˚C. The error bars represent the standard deviation for the three replicates.

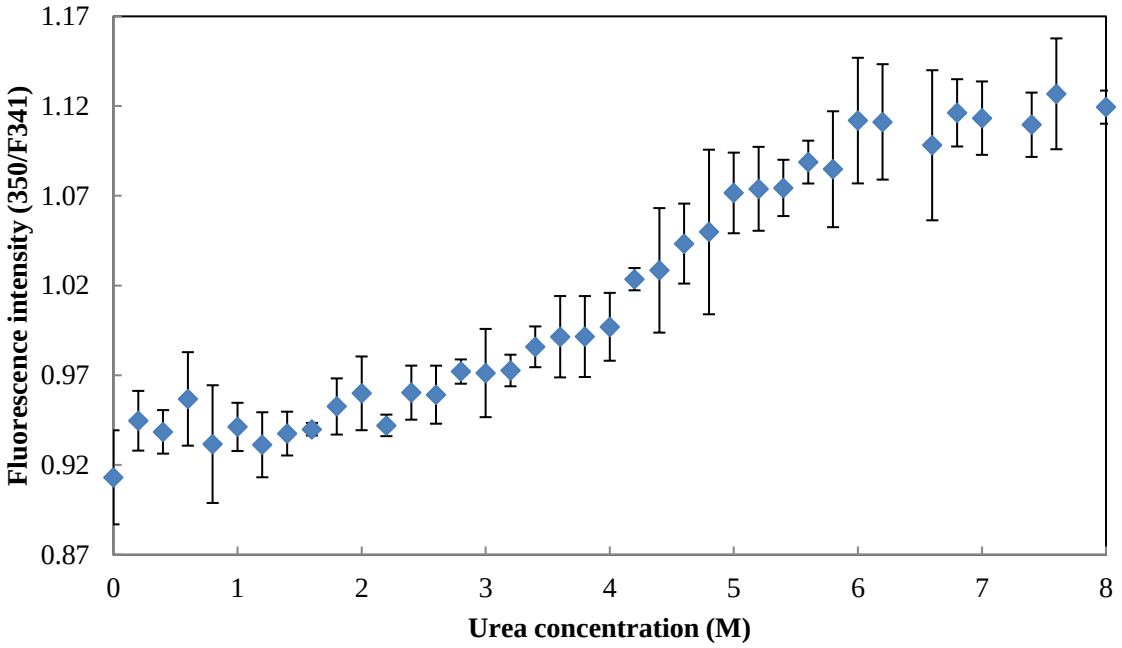

Figure 3.18: The unfolding of hGSTP1-1 using urea monitored by Trp fluorescence. F_{350}/F_{341} is the ratio of the fluorescence intensity for the unfolded protein (350 nm) to that of the native protein (341 nm) after the excitation of Trp residues at 295 nm. Unfolding of 2 μM of the protein was done in 5 mM sodium phosphate buffer, pH 6.5 at 20 ˚C. The experiment was done in triplicate and the error bars represent the standard deviation for the replicates.

CHAPTER 4
DISCUSSION

The aim of this study was to characterise the structure, function and stability of human glutathione *S*-transferase (hGSTP1-1). The structure of the protein was characterised using SDS-PAGE, UV-Visible spectroscopy, far-UV circular dichroism, intrinsic Trp fluorescence and size-exclusion high performance liquid chromatography. The function of hGSTP1-1 was characterised using ANS-binding studies and a GSH-CDNB conjugation assay. The stability of the protein was determined using thermal unfolding and urea-denaturation studies. Characterising hGSTP1-1 is important because the protein has an important role as a Phase II detoxification enzyme, regulation of the MAP kinase pathway (Adler *et al.* 1999), protecting cells from nitrosative stress (Klatt *et al.*, 1999) and regulating the function of 1-Cys peroxiredoxin (Manevich *et al.*, 2004).

Prokaryotic expression systems such as *Escherichia coli* are usually used to produce large quantities of heterologous proteins for structural and functional studies (Itakura *et al*., 1977). Despite the many advantages of heterologous protein expression, there are also a few factors that have to be taken into consideration in order to maximise the likelihood of high protein expression. The vector with the insert of the desired protein might contain codons that are scarcely used in *E.coli*, resulting in the synthesis of low levels of the heterologous proteins (Kane, 1995) and the presence of missense substitutions in the synthesised protein (Parker, 1989). This codon bias is usually overcome by codon harmonisation, which entails the modification of rare codons in the target gene so that they more closely mirror the codon usage of the host, without altering the amino acid sequence of the protein which is encoded (Kink *et al*., 1991; Nambiar *et al*., 1984). Some vectors may also contain regulatory elements that limit protein expression within the coding sequence, resulting in low yields of the heterologous protein (Gustafsson *et al*., 2012). Properly-designed prokaryotic expression vectors have to contain a set of optimally arranged genetic elements that influence aspects that relate to the transcription and translation of protein expression. In addition to this, the origin or replication (Ori) determines the copy number, while including an antibiotic-resistance gene facilitates the phenotypic selection of the vector, (Figurski and Helsinki, 1979).

The pET-15b vector that was used in this study has a carbenicillin-resistance gene which is used as a selectable marker and a strong T7 promoter which is capable of producing large quantities of hGSTP1-1 in a simple and cost-effective manner (Dubendorf and Studier, 1991).

Induction of protein expression only requires 0.2 mM of isopropyl-β-D-thiogalactopyranoside (IPTG) and 37 °C for 6 hours. The T7 promoter also exhibits a minimal level of basal expression, since the lac repressor blocks the promoter in the absence of IPTG (Dubendorf and Studier, 1991). The common drawback of thermally inducible gene expression is that it results in the induction of the heat-shock response and the accompanying upregulation of proteases (Sonna *et al*., 2002). Using T7 Express Competent *E.coli* cells minimised this problem because the cells are naturally deficient of the *Ion* and *ompT* proteases which are present in other strains and are responsible for the degradation of misfolded protein and preventing the accumulation of some cell cycle-specific proteins (Grodberg and Dunn, 1988). The recombinant protein partitioned into the soluble fraction, which is indicative of a stably folded recombinant protein and would most likely be fully functional.

Affinity tags are usually used during the generation of recombinant proteins because they aid the purification of proteins and rarely affect the structure and biological function of the protein to which they are attached (Uhlén *et al*., 1992). hGSTP1-1 was expressed with an N-terminal hexahistidine tag that would allow the protein to be purified by Ni^{2+} immobilised metal affinity chromatography (IMAC), which is one of the simplest and most effective protein purification methods (Porath, 1992). The use of N-terminal hexahistidine tag ensures that the bacterial transcriptional and translational machineries always encounter N-terminal and 5' sequences that are compatible with strong RNA synthesis and protein expression, respectively. Histidine tags are also relatively small and do not substantially affect the solubility of the target protein, which usually happens with larger tags such as the maltose-binding protein (MBP)(Nallamsetty and Waugh, 2006; Nallamsetty and Waugh, 2007; Waugh, 2005).

IMAC was used for the production of pure hGSTP1-1. The technique has the advantages of having specific, strong binding which ensures that the His-tagged protein remains bound to the column during washing; mild elution conditions that do not perturb the integrity of the protein; and the ability to control selectivity of binding to the column by including low concentrations (50 mM) of imidazole to the equilibration buffer (Porath, 1992). The inclusion of NaCl in the equilibration and wash buffers maintains the solubility and stability of the protein by eliminating ion exchange effects (Porath, 1992). High concentrations (300 mM) of imidazole are used to competitively elute the His-tagged hGSTP1-1 from the column. Dialysis into 20 mM sodium phosphate buffer, pH 7.4, with 0.02% NaN_3 and 2 mM DTT was done to remove imidazole from the purified protein solution, since the compound interferes with protein quantitation and other downstream applications (Molina *et al*., 1996).

GSTs are enzymes that catalyse the addition of glutathione (GSH) to substrates that have electrophilic functional groups (Armstrong, 1991, 1994; Habig and Jakoby, 1981; Habig *et al*., 1974). This reaction is sequential, with the addition only occurring in the ternary complex of the enzyme, GSH and an electrophile such as 1-chloro-2,4-dinitrobenzene (CDNB). Before the reaction starts, CDNB binds to the H-site of the enzyme, while GSH binds to the G-site. A neighbouring tyrosine residue (Tyr7) on hGSTP1-1 removes the proton from the thiol of GSH by lowering the pK_a of the bound thiol, thus allowing ionisation to occur at physiological pH (Prade *et al*., 1997; Shishido *et al*., 2017). The highly nucleophilic thiolate anion (GS^-) which is formed in the process has been shown to be up to 10^9 times more reactive than its conjugate acid (Roberts *et al*., 1986). This anion is responsible for attacking the electrophilic CDNB to produce the GS-DNB conjugate as shown in Figure 4.1. The Meisenheimer complex that is also shown in the figure is a complex of 1-chloro-2,4-dinitrobenzene and GSH that portrays a classical example for the transition state σ-complex after the nucleophilic substitution that occurs at the aromatic ring (Shishido *et al*., 2017).

The difference in the structure of the G-site in different subtypes of GST enzymes makes it possible to design subtype-selective inhibitors. Competitive inhibition of GST enzymes by targeting the G-site would result in a decrease in their apparent affinity to GSH and an increase in the K_m, while the V_{max} would remain the same (Reed *et al*., 2010). The specific activity of hGSTP1-1 that was obtained in this study (55.5 μmol/min/mg) is in the range of 33 μmol/min/mg to 75 μmol/min/mg that has been reported in the literature (Goodrich and Basu, 2012; Habig *et al*., 1974; Huang *et al*., 2008). Inhibition of hGSTP1-1 is a promising approach to the treatment of cancer since it would make cancerous cells more sensitive to chemotherapy (Laborde, 2010; Sau *et al*., 2010). A number of GSH derivatives that competitively inhibit different GST enzymes by binding to the G-site have already been reported (Kunze and Heps, 2000; Lyttle *et al*., 1994; Mahajan and Atkins, 2005; Nakajima *et al*., 2003).

The problem with using GSH derivatives as inhibitors is that continuous or high-dose administration of the inhibitor is necessary to compete with the high concentrations of GSH (1-10 mM) in cells (Lushchak, 2012). A better approach that is recently being explored is to design covalent inhibitors that bind to the G-site to provide sustained and strong inhibition and selectivity. Some of these inhibitors have been shown to be stronger inhibitors than some commercially available inhibitors such as *S*-hexyl GSH based on their IC_{50} values (Shishido *et al*., 2017).

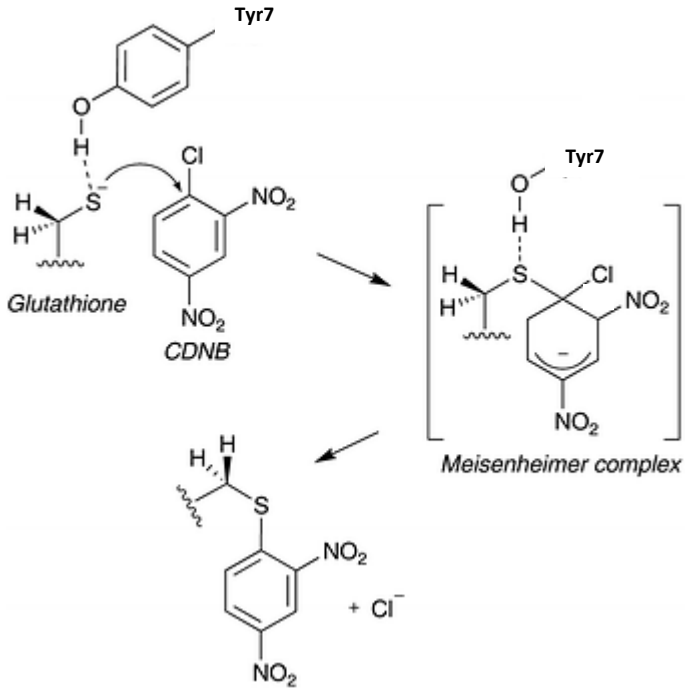

Figure 4.1: The reaction pathway resulting in the formation of a GS-DNB conjugate. The sulphur atom of glutathione is initially hydrogen bonded to Try7 and to a water molecule. The dinitrobenzene moiety then occupies the place of the water molecule in the Meisenheimer complex, allowing the sulphur to attack the CDNB. A covalent bond is formed after proton transfer to the water molecule (van der Kamp and Mulholland, 2008).

Analysis of the secondary structure of hGSTP1-1 using far-UV circular dichroism shows a spectrum with minimum ellipticity values at 208 nm and 222 nm (Figure 3.11), which is indicative of a protein which is predominantly alpha helical (Sreerama and Woody, 2000). This is consistent with other findings from other studies and what has been observed in crystal structures of the protein (Dirr *et al*., 1994; Gildenhuys *et al*., 2010; Ji *et al*., 1997; Oakley *et al*., 1998). The two subunits in hGSTP1-1 are made up of two domains that are non-identical (Ji *et al*., 1997). The first domain (amino acid residues 1-76) has the only two tryptophan residues at positions 28 and 38 of the amino acid sequence and also has 37 % of the total secondary structure of the protein. There are a total of 31 amino acid residues in α-helices and 18 residues in β-strands. The second domain (amino acid residues 82-209) has 63 % of the total secondary structure , with 82 amino acid residues forming α-helices and no residues forming β-strands. Figure 4.2 is a crystal structure of the apo form of hGSTP1-1 (PDB code: 16GS), coloured according to the two separate subunits (Oakley *et al*., 1998).

Solid state studies conducted using freeze-dried proteins to investigate the relative stability of α-helices and β-sheets have shown that proteins that have a high alpha helical content are generally less stable than those that have a higher number of beta sheets (Henzler Wildman *et al*., 2002). This, however, is in contrast with a liquid environment which favours the formation of α-helices.

Tryptophan residues, which are the dominant intrinsic fluorophore in protein molecules, were used to characterise the tertiary structure of hGSTP1-1. After excitation at 295 nm, the emission maximum occurred at 343 nm in 5 mM sodium phosphate buffer, pH 7.4. This emission spectrum is largely dependent on the polarity of the solvent since the formation of hydrogen bonds between the solvent and tryptophan residues determines the wavelength of maximum emission (Burstein *et al*., 1973; Lasser *et al*., 1977; Meng *et al*., 2013). Since hGSTP1-1 has two tryptophan residues (Trp28 and Trp38) which are both partially exposed to the solvent, the emission spectrum that was obtained reflects the average environment of both residues (Reinemer *et al*., 1992).

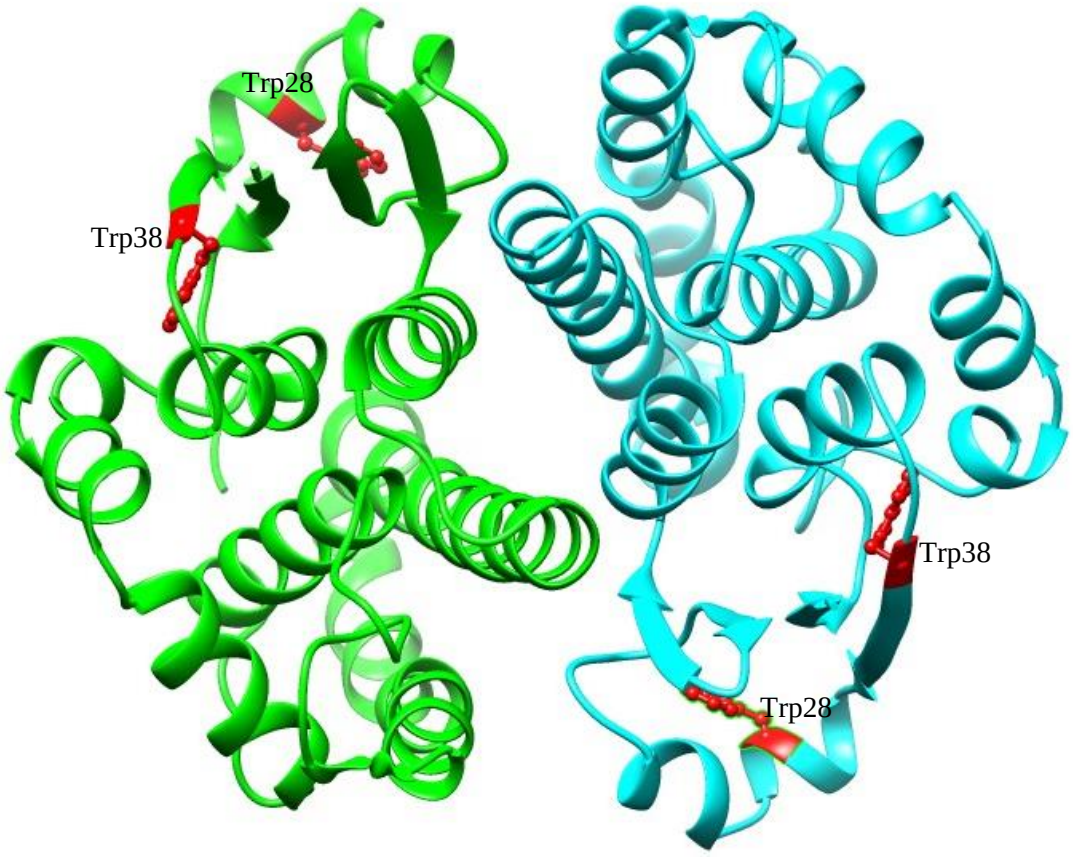

Figure 4.2: A crystal structure of the apo form of hGSTP1-1 (PDB code: 16GS). The Each subunit of the homodimer has two domains. Domain 1 has the two tryptophan residues (shown as ball and stick models in red) and 37% of the secondary structure of the protein, while domain 2 has 63 % of the secondary structure of the protein. hGSTP1-1 has 114 residues forming α helices and 18 residues forming β strands. Adapted from Oakley *et al.* (1998).

The quaternary structure of hGSTP1-1 that was obtained in this study is different from findings that have been reported in the literature. Since the protein is too unstable to exist as a monomer, other studies have shown that it can only exist as a folded dimer or an unfolded monomer, without a stable monomeric intermediate (Erhardt and Dirr, 1996; Gildenhuys *et al*., 2010). A folded monomer of hGSTP1-1 has molecular mass of 23.5 kDa (Kano *et al*., 1987; Mannervik, 1985), which is very similar to what was obtained in this study (23.9 kDa). Since the protein sample that was analysed using SE-HPLC had not been concentrated, this may have affected the apparent molecular mass of the native protein. It has been shown in other studies that due to the low resolution of SE-HPLC, using low concentrations of protein can generate artifactual low molecular mass estimations that can easily be misinterpreted as a signal of the formation of monomeric structures (Fabrini *et al*., 2009). When characterisation of the protein was done by Gildenhuys and Dirr (1996) and Gildenhuys *et al* (2010), the protein was in a buffer solution with 0.1 M NaCl. However, the buffer system that was used in this study contained a much higher concentration of salt (0.5 M) and had a higher pH (8) than the pI of the protein (5.4). This gave the protein a net negative charge from the strongly hydroxylated side chains on Asp and Glu. Monovalent cations of Na^+ are less effective than multivalent ions in weakening repulsive electrostatic intermolecular interactions than multivalent cations according to the reverse Hofmeister series (Ries-Kautt and Ducruix, 1989). The anions in the solution bind to the weakly hydrated sites on the protein more strongly than the interactions between Na^+ ions and carboxylate groups, which would effectively increase the repulsive interactions between the subunits of hGST-P1 resulting in the formation of monomers. This is consistent with experimental findings for protein-protein interactions of ovalbumin in NaCl at pH conditions above its pI (Ianeselli *et al*., 2010).

The way that the fluorescence of 8-anilinonaphthalene-1-sulfonic acid (ANS) changes when it binds to hGSTP1-1 is similar to what has been observed when the dye binds to other proteins (Cardamone and Puri, 1992; Kinsley *et al*., 2008). Studies done on different classes of GSTs have shown that the site of binding is the region that is near or at the active site (H-site) and the dimer interface (Dirr *et al*., 2005; Kinsley *et al*., 2008; Ralat and Colman, 2004). The naphthalene ring system becomes buried inside the H-site pocket, while the aniline group is exposed and more dynamic (Kinsley *et al*., 2008). It has also been shown that the dye does not bind unfolded glutathione *S*-transferases (Dirr and Wallace, 1999; Yassin *et al*., 2004)

Previous studies that have been done using titration calorimetry have shown that the binding of ANS to most proteins involves the formation of ion pairs between the negatively charged

sulfonate group of ANS and cationic groups on the protein molecules (Matulis *et al*., 1999; Matulis and Lovrien, 1998). The establishment of these electrostatic forces would cause the protein to adopt a more compact structure than the one that existed before ANS binding (Matulis *et al*., 1999). Although this is true for most proteins, studies have also shown that the binding of ANS to GST proteins does not affect their conformational stability (Bico *et al*., 1995; Wallace and Dirr, 1999; Yassin *et al*., 2004), which means that the amount of bound ANS is an accurate reflection of the number of hydrophobic patches on hGSTP1-1.

The thermal unfolding of hGSTP1-1 was found to be an irreversible process, since there was no decrease in the ellipticity at 222 nm when the protein sample was cooled from 80 ˚C to 20˚C (Figure 3.14). This irreversibility is probably a consequence of the formation of aggregates when the protein is exposed to high temperatures (Benjwal *et al*., 2006). High temperatures (that increase the stress experienced by live cells) cause proteins to misfold, leading to the formation of aggregates that are toxic to the cells. When cells are exposed to high temperatures, they start to synthesise heat shock proteins such as chaperones to mitigate the accumulation of aggregates (Ellis and van der Vies, 1991). These chaperones prevent any newly synthesised proteins and assembled units from aggregating into non-functional structures (Verghese *et al*., 2012). Figure 3.14 also does not show the presence of a stable intermediate during the unfolding of hGSTP1-1. This implies that the protein follows a two-state folding model.

The intrinsic fluorescence of hGSTP1-1 was used to monitor any changes in the tertiary structure of the protein during unfolding because of the high sensitivity of tryptophan residues to their local environment. Any apparent changes in the emission spectra of tryptophan are usually as a result of substrate binding (Wang *et al*., 2009), denaturation (Gildenhuys *et al*., 2010), subunit association or conformational transitions (Khan *et al*., 2016). When unfolded hGSTP1-1 was refolded by performing a five-fold dilution of the protein in 8 M urea, the Trp fluorescence emission spectrum did not overlay with that of the control (Figure 3.15B). The λ_{max} for the two samples only differed by 1 nm (343 nm for the control vs 344 nm for the recovered protein sample), which means that the tryptophan residues in the two samples were in near-identical environments (Kronman and Holmes, 1971; Teale, 1960). The 84 % recovery of the denatured enzyme that was obtained is very close to the 85 % recovery that has been obtained in other studies involving hGSTP1-1 (Erhardt and Dirr, 1996).

When hGSTP1-1 was denatured using 8 M urea, there was a shift in λ_{max} from 343 nm (for the native protein) to 350 nm (for the completely unfolded protein), indicating that the two

tryptophan residues in each subunit had become completely exposed to the aqueous solvent (Aceto *et al*., 1992). These findings are consistent with what has been reported in other studies which showed that the exposure of tryptophan residues to water results in a shift in the emission to longer wavelengths (Burstein *et al*., 1973; Chen& Rhoades, 2008; Gildenhuys *et al*., 2010). The increase in the fluorescence intensity that was observed as the protein unfolded is also consistent with stability studies involving GSTP1-1 that have been reported in the literature (Erhardt and Dirr, 1996; Gildenhuys *et al*., 2010).

Since most of the α-helices (63 %) in hGSTP1-1 are located in domain 2 (Prade *et al*., 1997; Reinemer *et al*., 1992), measurements of the ellipticity at 222 nm during unfolding principally gives an indication of conformational modifications in this domain. Fluorescence measurements, in contrast, are used to monitor changes in the structures surrounding Trp28 and Trp38 in domain 1. Almost half of the change in tryptophan fluorescence that is observed during unfolding of hGSTP1-1 happens at low concentrations of urea (1 M to 3.8 M), which is not accompanied by any drastic changes in the secondary structure of the protein (Figure 3.15 and Figure 3.17). This is an indication that domain 1 is less stable than domain 2 and its structure begins to change before domain 2 unfolds. This is an important structural feature of the enzyme, since too much stability would adversely affect its function (Shoichet *et al*., 1995). The low stability of domain 1 allows for movements that can occur quickly during GSH binding, since there is a low energy barrier for transition between different conformational states (Gerstein *et al*., 1994). When the concentration of urea is increased further (between 3.8 M and 5.4 M), there is a decrease in the fluorescence intensity which is accompanied by a loss of the secondary structure. This suggests that the unfolding of domain 1 is somehow dependent on domain 2 and both domains behave as a single cooperative unit (Gildenhuys *et al*., 2010). The post transition region between 5.4 M and 8 M urea (Figure 3.15) coincides with an increase in the fluorescence intensity, which also suggests that the concentration of urea also has some influence on the fluorescence intensity. This is consistent with other studies that have shown that denaturing concentrations of urea can increase the yield of tryptophan fluorescence by up to 20 % when compared with denaturants such as guanidinium hydrochloride (Kronman and Holmes, 1971). The effect of urea on the fluorescence signal can also be seen in Figure 3.17, which shows a drastic increase in the fluorescence signal of hGSTP1-1 between 0 M and 1 M urea.

There is evidence for two contrasting pathways that can be used to describe the unfolding of GSTP1-1. One study discovered that the denaturation of hGSTP1-1 occurs in two steps and

involves the dissociation of an active dimer into monomers that are structured but inactive before complete unfolding occurs (Aceto *et al*., 1992). Other studies found that the unfolding of both human and porcine GSTP1-1 resembles a concerted two-state process with only the native dimer which is active and the completely unfolded monomers without any stable intermediate (Dirr and Reinemer, 1991; Gildenhuys *et al*., 2010). The unfolding curve of hGSTP1-1 that was obtained in this study (Figure 3.18) shows that the protein unfolds cooperatively via a two-state model, which is consistent with the findings of Dirr and Reinemer (1991) and Gildenhuys *et al* (2010). According to the unfolding curve of hGSTP1-1 shown in Figure 3.18, the transition midpoint of the protein is 4.6 M urea, which is the same as the value that has been obtained in other studies (Erhardt and Dirr, 1996).

Conclusion

The results obtained in this study were consistent with information that has previously been reported in literature, except for the characterisation of the quaternary structure of hGSTP1-1. However, since there is no other specie apart from the 24 kDa peak that was observed in the SE-HPLC chromatogram, it can be concluded that if the protein does indeed form multi-subunit complexes, the subunits would be identical. Understanding how hGSTP1-1 behaves in different environments is important for drug design because it makes it possible to predict how the structure and consequently the function of the enzyme will be affected when a particular drug is administered.

REFERENCES

Abkevich, V.I., Gutin, A.M. and Shakhnovich, E.I., 1994. Specific nucleus as the transition state for protein folding: evidence from the lattice model. Biochemistry, 33(33), 10026-10036.

Aceto, A., Caccuri, A.M., Sacchetta, P. and Bucciarelli, T., Dragani, B., Rosato, N., Federici, G., Di Ilio, C., 1992. Dissociation and unfolding of Pi-class glutathione transferase. Evidence for a monomeric inactive intermediate. Biochemical Journal 285, 241-245.

Adler, V., Yin, Z., Fuchs, S.Y., Benezra, M., Rosario, L., Tew, K.D., Pincus, M.R., Sardana, M., Henderson, C.J., Wolf, C.R. and Davis, R.J., 1999. Regulation of JNK signaling by GSTp. The EMBO Journal, 18(5), 1321-1334.

Ahmad, H., Wilson, D.E., Fritz, R.R., Singh, S.V., Medh, R.D., Nagle, G.T., Awasthi, Y.C. and Kurosky, A., 1990. Primary and secondary structural analyses of glutathione S-transferase π from human placenta. Archives of Biochemistry and Biophysics, 278(2), 398-408.

Ali-Osman, F., Akande, O., Antoun, G., Mao, J.X. and Buolamwini, J., 1997. Molecular cloning, characterization, and expression in escherichia coli of full-length CDNAs of three human glutathione s-transferase Pi gene variants evidence for differential catalytic activity of the encoded proteins. Journal of Biological Chemistry, 272(15), 10004-10012.

Altschul, S.F., Gish, W., Miller, W., Myers, E.W., and Lipman, D.J., 1990. Basic local alignment search tool. Journal of Molecular Biology 215, 403-410.

Alves, C.S., Kuhnert, D.C., Sayed, Y. and Dirr, H.W., 2006. The intersubunit lock-and-key motif in human glutathione transferase A1-1: role of the key residues Met51 and Phe52 in function and dimer stability. Biochemical Journal, 393(2), 523-528.

Anfinsen, C.B., 1973. Principles that govern the folding of protein chains. Science, 181(4096), pp.223-230.

Armstrong, R.N., 1991. Glutathione S-transferases: reaction mechanism, structure, and function. Chemical Research in Toxicology 4, 131-140.

Armstrong, R.N., 1994. Glutathione S-transferases: structure and mechanism of an archetypical detoxication enzyme. Advances in Enzymology and Related Areas of Molecular Biology 69, 1-44.

Asakura, T., Hashizume, Y., Tashiro, K.I., Searashi, Y., Ohkawa, K., Nishihira, J., Sakai, M. and Shibasaki, T., 2001. Suppression of GST-P by treatment with glutathione-doxorubicin conjugate induces potent apoptosis in rat hepatoma cells. International Journal of Cancer, 94(2), 171-177.

Ateş, N.A., Tamer, L., Ateş, C., Ercan, B., Elipek, T., Öcal, K. and Çamdeviren, H., 2005. Glutathione S-transferase M1, T1, P1 genotypes and risk for development of colorectal cancer. Biochemical Genetics, 43(3), 149-163.

Atkins, W.M., Wang, R.W., Bird, A.W., Newton, D.J. and Lu, A.Y., 1993. The catalytic mechanism of glutathione S-transferase (GST). Spectroscopic determination of the pKa of Tyr-9 in rat alpha 1-1 GST. Journal of Biological Chemistry, 268(26), 19188-19191.

Balchin, D., Wallace, L. and Dirr, H.W., 2013. S-nitrosation of glutathione transferase p1-1 is controlled by the conformation of a dynamic active site helix. Journal of Biological Chemistry, 288(21), 14973-14984.

Balchin, D., Stoychev, S.H. and Dirr, H.W., 2013. S-Nitrosation destabilizes glutathione transferase P1-1. Biochemistry, 52(51), 9394-9402.

Banham, A.H., Boddy, J., Launchbury, R., Han, C., Turley, H., Malone, P.R., Harris, A.L. and Fox, S.B., 2007. Expression of the forkhead transcription factor FOXP1 is associated both with hypoxia inducible factors (HIFs) and the androgen receptor in prostate cancer but is not directly regulated by androgens or hypoxia. The Prostate, 67(10), 1091-1098.

Bello, M.L., Nuccetelli, M., Chiessi, E., Lahm, A., Mazzetti, A.P., Battistoni, A., Caccuri, A.M., Oakley, A.J., Parker, M.W., Tramontano, A. and Federici, G., 1998. Mutations of Gly to Ala in human glutathione transferase P1-1 affect helix 2 (G-site) and induce positive cooperativity in the binding of glutathione. Journal of Molecular Biology, 284(5), 1717-1725.

Benjwal, S., Verma, S., Röhm, K.H. and Gursky, O., 2006. Monitoring protein aggregation during thermal unfolding in circular dichroism experiments. Protein Science 15, 635-639.

Bernardini, S., Bernassola, F., Cortese, C., Ballerini, S., Melino, G., Motti, C., Bellincampi, L., Iori, R. and Federici, G., 2000. Modulation of GST P1-1 activity by polymerization during apoptosis. Journal of Cellular Biochemistry, 77(4), 645-653.

Bico, P., Erhardt, J., Kaplan, W. and Dirr, H., 1995. Porcine class pi glutathione S-transferase: anionic ligand binding and conformational analysis. Biochimica et biophysica acta 1247, 225-230.

Board, P.G., Webb, G.C. and Coggan, M., 1989. Isolation of a cDNA clone and localization of the human glutathione S-transferase 3 genes to chromosome bands 11q13 and 12q13-14. Annals of Human Genetics, 53(3), 205-213.

Boese, M., Keese, M.A., Becker, K., Busse, R. and Mülsch, A., 1997. Inhibition of glutathione reductase by dinitrosyl-iron-dithiolate complex. Journal of Biological Chemistry, 272(35), 21767-21773.

Boyland, E. and Chasseaud, L.F., 1967. Enzyme-catalysed conjugations of glutathione with unsaturated compounds. Biochemical Journal, 104(1), 95.

Bryngelson, J.D., Onuchic, J.N., Socci, N.D. and Wolynes, P.G., 1995. Funnels, pathways, and the energy landscape of protein folding: a synthesis. Proteins: Structure, Function, and Bioinformatics, 21(3), 167-195.

Burstein, E.A., Vedenkina, N.S. and Ivkova, M.N., 1973. Fluorescence and the location of tryptophan residues in protein molecules. Photochemistry and Photobiology 18, 263-279.

Cardamone, M., Puri, N.K., 1992. Spectrofluorimetric assessment of the surface hydrophobicity of proteins. The Biochemical Journal 282 (Pt 2), 589-593.

Chen, Y.R., Wang, X., Templeton, D., Davis, R.J. and Tan, T.H., 1996. The role of c-Jun N-terminal kinase (JNK) in apoptosis induced by ultraviolet C and γ radiation duration of JNK activation may determine cell death and proliferation. Journal of Biological Chemistry, 271(50), 31929-31936.

Chen, H. and Jachau, M.R., 1998. Recombinant human glutathione S-transferases catalyse enzymic isomerization of 13-cis-retinoic acid to all-trans-retinoic acid in vitro. Biochemical Journal, 336(1), 223-226.

Chen, H. and Rhoades, E., 2008. Fluorescence characterization of denatured proteins. Current Opinion in Structural Biology 18, 516-524.

Chung, C.T., Niemela, S.L. and Miller, R.H., 1989. One-step preparation of competent Escherichia coli: transformation and storage of bacterial cells in the same solution. Proceedings of the National Academy of Sciences, 86(7), 2172-2175.

Cookson, M.S., Reuter, V.E., Linkov, I. and Fair, W.R., 1997. Glutathione S-transferase Pi (GST-pi) class expression by immunohistochemistry in benign and malignant prostate tissue. The Journal of Urology, 157(2), 673-676.

Dirr, H., Reinemer, P. and Huber, R., 1994. X-ray crystal structures of cytosolic glutathione S-transferases. Implications for protein architecture, substrate recognition and catalytic function. European Journal of Biochemistry 220, 645-661.

Dirr, H.W., Little, T., Kuhnert, D.C. and Sayed, Y., 2005. A conserved N-capping motif contributes significantly to the stabilization and dynamics of the C-terminal region of class Alpha glutathione S-transferases. The Journal of Biological Chemistry 280, 19480-19487.

Dirr, H.W. and Reinemer, P., 1991. Equilibrium unfolding of class pi glutathione S-transferase. Biochemical and Biophysical Research Communications 180, 294-300.

Dirr, H.W. and Wallace, L.A., 1999. Role of the C-terminal helix 9 in the stability and ligandin function of class alpha glutathione transferase A1-1. Biochemistry 38, 15631-15640.

Dubendorf, J.W. and Studier, F.W., 1991. Controlling basal expression in an inducible T7 expression system by blocking the target T7 promoter with lac repressor. Journal of Molecular Biology, 219(1), 45-59.

Ellis, R.J. and van der Vies, S.M., 1991. Molecular chaperones. Annual Review of Biochemistry 60, 321-347.

Erhardt, J. and Dirr, H., 1996. Effect of glutathione, glutathione sulphonate and S-hexylglutathione on the conformational stability of class pi glutathione S-transferase. FEBS Letters 391, 313-316.

Fabrini, R., De Luca, A., Stella, L., Mei, G., Orioni, B., Ciccone, S., Federici, G., Lo Bello, M. and Ricci, G., 2009. Monomer− dimer equilibrium in glutathione transferases: a critical re-examination. Biochemistry, 48(43), 10473-10482.

Faulder, C. G., Hirrell, P. A., Hume, R. and Strange, R. C., 1987. Studies of the development of basic, neutral and acidic isoenzymes of glutathione S-transferase in human liver, adrenal, kidney and spleen. Biochemical Journal, 241(1), 221-228.

Figurski, D.H. and Helinski, D.R., 1979. Replication of an origin-containing derivative of plasmid RK2 dependent on a plasmid function provided in trans. Proceedings of the National Academy of Sciences, 76(4), 1648-1652.

Gallagher, E.P., Gardner, J.L., **Barber, D.S.**, 2006. Several glutathione S-transferase isozymes that protect against oxidative injury are expressed in human liver mitochondria. Biochemical Pharmacology, 71(11), 1619-1628.

Gasteiger, E., Hoogland, C., Gattiker, A., Wilkins, M.R., Appel, R.D. and Bairoch, A., 2005. Protein identification and analysis tools on the ExPASy server. The proteomics protocols handbook, 571-607. Humana press.

Gerstein, M., Lesk, A.M. and Chothia, C., 1994. Structural mechanisms for domain movements in proteins. Biochemistry, 33(22), 6739-6749.

Gildenhuys, S., Wallace, L.A., Burke, J.P., Balchin, D., Sayed, Y., Dirr, H.W., 2010. Class Pi glutathione transferase unfolds via a dimeric and not monomeric intermediate: functional implications for an unstable monomer. Biochemistry 49, 5074-5081.

Glasel, J.A., 1995. Validity of nucleic acid purities monitored by 260nm/280nm absorbance ratios. BioTechniques 18, 62-63.

Goodrich, J.M. and Basu, N., 2012. Variants of glutathione s-transferase Pi 1 exhibit differential enzymatic activity and inhibition by heavy metals. Toxicology in Vitro 26, 630-635.

Goto, S., Kawakatsu, M., Izumi, S.I., Urata, Y., Kageyama, K., Ihara, Y., Koji, T. and Kondo, T., 2009. Glutathione S-transferase π localizes in mitochondria and protects against oxidative stress. Free Radical Biology and Medicine, 46(10), 1392-1403.

Gottesman, M.M. and Pastan, I., 1993. Biochemistry of multidrug-resistance mediated by the multidrug transporter. Annual Review of Biochemistry 62, 385–427

Greenfield, N.J. and Fasman, G.D., 1969. Computed circular dichroism spectra for the evaluation of protein conformation. Biochemistry, 8(10), 4108-4116.

Grodberg, J. and Dunn, J.J., 1988. ompT encodes the Escherichia coli outer membrane protease that cleaves T7 RNA polymerase during purification. Journal of Bacteriology, 170(3), 1245-1253.

Gustafsson, C., Minshull, J., Govindarajan, S., Ness, J., Villalobos, A. and Welch, M., 2012. Engineering genes for predictable protein expression. Protein Expression and Purification, 83(1), 37-46.

Guthenberg, C., Warholm, M., Rane, A. and Mannervik, B., 1986. Two distinct forms of glutathione transferase from human foetal liver. Purification and comparison with isoenzymes isolated from adult liver and placenta. Biochemical Journal, 235(3), 741-745.

Habig, W.H., Jakoby, W.B., 1981. Assays for differentiation of glutathione S-transferases. Methods in Enzymology 77, 398-405.

Habig, W.H., Pabst, M.J. and Jakoby, W.B., 1974. Glutathione *S*-transferases. The first enzymatic step in mercapturic acid formation. The Journal of Biological Chemistry 249, 7130-7139.

Hayes, J.D., and Pulford, D.J., 1995. The glutathione *S*-transferase supergene family: regulation of GST and the contribution of the lsoenzymes to cancer chemoprotection and drug resistance part II. Critical Reviews in Biochemistry and Molecular Biology, 30(6), 521-600.

Heijn, M., Oude Elferink, R.P.J. and Jansen, P.M.L., 1992. ATP-dependent multispecific organic anion transport system in rat erythrocyte membrane vesicles. American Journal of Physiology 262, C104–C110

Henzler Wildman, K.A., Lee, D.K. and Ramamoorthy, A., 2002. Determination of alpha-helix and beta-sheet stability in the solid state: a solid-state NMR investigation of poly(L-alanine). Biopolymers 64, 246-254.

Hill, B.G., Ramana, K.V., Cai, J., Bhatnagar, A. and Srivastava, S.K., 2010. Measurement and identification of S-glutathiolated proteins. Methods in Enzymology, 473, 179-197.

Howells, R.E.J., Dhar, K.K., Hoban, P.R., Jones, P.W., Fryer, A.A., Redman, C.W.E. and Strange, R.C., 2004. Association between glutathione-S-transferase GSTP1 genotypes, GSTP1 over-expression, and outcome in epithelial ovarian cancer. International Journal of Gynecological Cancer, 14(2), 242-250.

Hu, X., Herzog, C., Zimniak, P. and Singh, S.V., 1999. Differential protection against benzo [a] pyrene-7, 8-dihydrodiol-9, 10-epoxide-induced DNA damage in HepG2 cells stably transfected with allelic variants of π class human glutathione S-transferase. Cancer Research, 59(10), 2358-2362.

Huang, J., Tan, P.H., Thiyagarajan, J. and Bay, B.H., 2003. Prognostic significance of glutathione S-transferase-pi in invasive breast cancer. Modern Pathology, 16(6), 558-565.

Huang, Y.C., Misquitta, S., Blond, S.Y., Adams, E. and Colman, R.F., 2008. Catalytically active monomer of glutathione S-transferase Pi and key residues involved in the electrostatic interaction between subunits. The Journal of Biological Chemistry 283, 32880-32888.

Ianeselli, L., Zhang, F., Skoda, M.W., Jacobs, R.M., Martin, R.A., Callow, S., Prevost, S. and Schreiber, F., 2010. Protein-protein interactions in ovalbumin solutions studied by small-angle scattering: effect of ionic strength and the chemical nature of cations. The Journal of Physical Chemistry. B 114, 3776-3783.

Ip, Y.T. and Davis, R.J., 1998. Signal transduction by the c-Jun N-terminal kinase (JNK)—from inflammation to development. Current Opinion in Cell Biology, 10(2), pp.205-219.

Isenberg, J.S., Martin-Manso, G., Maxhimer, J.B. and Roberts, D.D., 2009. Regulation of nitric oxide signalling by thrombospondin 1: implications for anti-angiogenic therapies. Nature Reviews Cancer, 9(3), 182-194.

Ishikawa, T., 1992. The ATP-dependent glutathione S-conjugate export pump. Trends in Biochemical Sciences 17, 463–468.

Itakura, K., Hirose, T., Crea, R., Riggs, A.D., Heyneker, H.L., Bolivar, F. and Boyer, H.W., 1977. Expression in Escherichia coli of a chemically synthesized gene for the hormone somatostatin. Science, 198(4321), 1056-1063.

Ji, X., Tordova, M., O'Donnell, R., Parsons, J.F., Hayden, J.B., Gilliland, G.L. and Zimniak, P., 1997. Structure and function of the xenobiotic substrate-binding site and location of a potential non-substrate-binding site in a class pi glutathione S-transferase. Biochemistry 36, 9690-9702.

Johansson, A.S., Stenberg, G., Widersten, M. and Mannervik, B., 1998. Structure-activity relationships and thermal stability of human glutathione transferase P1-1 governed by the H-site residue 105. Journal of Molecular Biology, 278(3), 687-698.

Kamada, K., Goto, S., Okunaga, T., Ihara, Y., Tsuji, K., Kawai, Y., Uchida, K., Osawa, T., Matsuo, T., Nagata, I. and Kondo, T., 2004. Nuclear glutathione S-transferase π prevents apoptosis by reducing the oxidative stress-induced formation of exocyclic DNA products. Free Radical Biology and Medicine, 37(11), 1875-1884.

Kane, J.F., 1995. Effects of rare codon clusters on high-level expression of heterologous proteins in Escherichia coli. Current Opinion in Biotechnology, 6(5), 494-500.

Kano, T., Sakai, M. and Muramatsu, M., 1987. Structure and expression of a human class pi glutathione S-transferase messenger RNA. Cancer research 47, 5626-5630.

Karin, M., 1995. The regulation of AP-1 activity by mitogen-activated protein kinases. Journal of Biological Chemistry, 270(28), 16483-16486.

Ketley, J.N., Habig, W.H., and Jakoby, W.B., 1975. Binding of nonsubstrate ligands to the glutathione S-transferases. Journal of Biological Chemistry, 250(22), 8670-8673.

Khan, P., Prakash, A., Haque, M.A., Islam, A., Hassan, M.I., Ahmad, F., 2016. Structural basis of urea-induced unfolding: Unraveling the folding pathway of hemochromatosis factor E. International Journal of Biological Macromolecules 91, 1051-1061.

Kim, Y.J., Lee, W.S., Ip, C., Chae, H.Z., Park, E.M. and Park, Y.M., 2006. Prx1 suppresses radiation-induced c-Jun NH2-terminal kinase signaling in lung cancer cells through interaction with the glutathione S-transferase Pi/c-Jun NH2-terminal kinase complex. Cancer Research, 66(14), 7136-7142.

Kink, J.A., Maley, M.E., Ling, K.Y., Kanabrocki, J.A. and Kung, C., 1991. Efficient Expression of the Paramecium Calmodulin Gene in Escherichia coli after Four TAA-to-CAA Changes through a Series of Polymerase Chain Reactions. Journal of Eukaryotic Microbiology, 38(5), 441-447.

Kinsley, N., Sayed, Y., Mosebi, S., Armstrong, R.N. and Dirr, H.W., 2008. Characterization of the binding of 8-anilinonaphthalene sulfonate to rat class Mu GST M1-1. Biophysical chemistry 137, 100-104.

Klatt, P., Molina, E.P. and Lamas, S., 1999. Nitric Oxide Inhibits c-Jun DNA Binding by Specifically Targeted S-Glutathionylation. Journal of Biological Chemistry, 274(22), 15857-15864.

Kobayashi, Y., 1999. A study on diagnosis of oral squamous cell carcinoma (oral SCC) by glutathione S-transferase-pi (GST-pi). Kokubyo Gakkai zasshi. The Journal of the Stomatological Society, Japan, 66(1), 46-56.

Kodym, R., Calkins, P., and Story, M., 1999. The Cloning and Characterization of a New Stress Response Protein: A mammalian member of a family of θ class glutathiones-transferase-like proteins. Journal of Biological Chemistry, 274(8), 5131-5137.

Komander, D. and Rape, M., 2012. The ubiquitin code. Annual Review of Biochemistry, 81, 203-229.

Koonin, E.V., Tatusov, R.L., Altschul, S.F., Bryant, S.H., Mushegian, A.R., Bork, P. and Valencia, A., 1994. Eukaryotic translation elongation factor 1γ contains a glutathione transferase domain—Study of a diverse, ancient protein super family using motif search and structural modeling. Protein Science, 3(11), 2045-2055.

Kronman, M.J. and Holmes, L.G., 1971. The fluorescence of native, denatured and reduced-denatured proteins*. Photochemistry and Photobiology 14, 113-134.

Kumar, S., Stecher, G. and Tamura, K., 2016. MEGA7: Molecular Evolutionary Genetics Analysis version 7.0 for bigger datasets. Molecular Biology and Evolution, 33(7), 1870-1874.

Kunze, T. and Heps, S., 2000. Phosphono analogs of glutathione: inhibition of glutathione transferases, metabolic stability, and uptake by cancer cells. Biochemical Pharmacology 59, 973-981.

Laborde, E., 2010. Glutathione transferases as mediators of signaling pathways involved in cell proliferation and cell death. Cell Death and Differentiation 17, 1373-1380.

Laemmli, U.K., 1970. Cleavage of structural proteins during the assembly of the head of bacteriophage T4. Nature, 227(5259), 680-685.

Lasser, N., Feitelson, J. and Lumry, R., 1977. Exciplex Formation between Indole Derivatives and Polar Solutes. Israel Journal of Chemistry 16, 330-334.

Leppä, S. and Bohmann, D., 1999. Diverse functions of JNK signaling and c-Jun in stress response and apoptosis. Oncogene, 18(45), 6158-6162.

Li, H., Helling, R., Tang, C. and Wingreen, N., 1996. Emergence of preferred structures in a simple model of protein folding. Science, 273(5275), 666.

Liu, S., Zhang, P., Ji, X., Johnson, W.W., Gilliland, G.L. and Armstrong, R.N., 1992. Contribution of tyrosine 6 to the catalytic mechanism of isoenzyme 3-3 of glutathione S-transferase. Journal of Biological Chemistry, 267(7), 4296-4299.

Lo Bello, M., Oakley, A.J., Battistoni, A., Mazzetti, A.P., Nuccetelli, M., Mazzarese, G., Rossjohn, J., Parker, M.W. and Ricci, G., 1997. Multifunctional role of Tyr 108 in the catalytic mechanism of human glutathione transferase P1-1. Crystallographic and kinetic studies on the Y108F mutant enzyme. Biochemistry, 36(20), 6207-6217.

Lushchak, V.I., 2012. Glutathione homeostasis and functions: potential targets for medical interventions. Journal of Amino Acids 2012, 736837.

Lyttle, M.H., Hocker, M.D., Hui, H.C., Caldwell, C.G., Aaron, D.T., Engqvist-Goldstein, A., Flatgaard, J.E. and Bauer, K.E., 1994. Isozyme-specific glutathione-S-transferase inhibitors: design and synthesis. Journal of Medicinal Chemistry 37, 189-194.

Mahajan, S. and Atkins, W.M., 2005. The chemistry and biology of inhibitors and pro-drugs targeted to glutathione S-transferases. Cellular and Molecular Life Sciences : CMLS 62, 1221-1233.

Manevich, Y., Sweitzer, T., Pak, J.H., Feinstein, S.I., Muzykantov, V. and Fisher, A.B., 2002. 1-Cys peroxiredoxin overexpression protects cells against phospholipid peroxidation-mediated membrane damage. Proceedings of the National Academy of Sciences, 99(18), 11599-11604.

Mannervik, B., 1985. The isoenzymes of glutathione transferase. Advances in Enzymology and Related Areas of Molecular Biology 57, 357-417.

Mannervik, B., AIlin, P., Guthenberg, C., Jensson, H., Tahir, M.K., Warholm, M. and Jornvall, H., 1985. Identification of three classes of cytosolic glutathione transferases common to several

mammalian species : Correlation between structural data and enzymatic properties. Proceedings of the National Academy of Sciences U.S.A. 82, 7202–7206

Mannervik, B., Castro, V.M., Danielson, U.H., Tahir, M.K., Hansson, J. and Ringborg, U., 1987. Expression of class Pi glutathione transferase in human malignant melanoma cells. Carcinogenesis, 8(12), 1929-1932.

Mannervik, B. and Danielson, U.H., 1988. Glutathione transferases--structure and catalytic activity. CRC Critical Reviews in Biochemistry 23, 283-337.

Mannervik, B., Awasthi, Y.C., Board, P.G., Hayes, J.D., Di Ilio, C., Ketterer, B., Listowsky, I., Morgenstern, R., Muramatsu, M. and Pearson, W.R. *et al.*, 1992. Nomenclature for human glutathione transferases. Biochemical Journal 282, 305–306

Matulis, D., Baumann, C.G., Bloomfield, V.A. and Lovrien, R.E., 1999. 1-anilino-8-naphthalene sulfonate as a protein conformational tightening agent. Biopolymers 49, 451-458.

Matulis, D. and Lovrien, R., 1998. 1-Anilino-8-naphthalene sulfonate anion-protein binding depends primarily on ion pair formation. Biophysical Journal 74, 422-429.

Meng, X., Harricharran, T. and Juszczak, L.J., 2013. A spectroscopic survey of substituted indoles reveals consequences of a stabilized 1Lb transition. Photochemistry and Photobiology 89, 40-50.

Molina, F., Rueda, A., Bosque-Sendra, J.M. and Megias, L., 1996. Determination of proteins in the presence of imidazole buffers. Journal of Pharmaceutical and Biomedical Analysis, 14(3), 273-280.

Muñoz, V., Blanco, F.J. and Serrano, L., 1995. The hydrophobic-staple motif and a role for loop-residues in α-helix stability and protein folding. Nature Structural & Molecular Biology, 2(5), 380-385.

Munoz, V. and Serrano, L., 1995. Analysis of i, i+ 5 and i, i+ 8 hydrophobic interactions in a helical model peptide bearing the hydrophobic staple motif. Biochemistry, 34(46), 15301-15306.

Nakajima, T., Takayama, T., Miyanishi, K., Nobuoka, A., Hayashi, T., Abe, T., Kato, J., Sakon, K., Naniwa, Y., Tanabe, H. and Niitsu, Y., 2003. Reversal of multiple drug resistance in cholangiocarcinoma by the glutathione S-transferase-pi-specific inhibitor O1-hexadecyl-gamma-glutamyl-S-benzylcysteinyl-D-phenylglycine ethylester. The Journal of Pharmacology and Experimental Therapeutics 306, 861-869.

Nallamsetty, S. and Waugh, D.S., 2006. Solubility-enhancing proteins MBP and NusA play a passive role in the folding of their fusion partners. Protein Expression and Purification, 45(1), 175-182.

Nallamsetty, S. and Waugh, D.S., 2007. A generic protocol for the expression and purification of recombinant proteins in Escherichia coli using a combinatorial His 6-maltose binding protein fusion tag. Nature Protocols, 2(2), 383.

Nambiar, K.P., Stackhouse, J., Stauffer, D.M., Kennedy, W.P., Eldredge, J.K. and Benner, S.A., 1984. Total synthesis and cloning of a gene coding for the ribonuclease S protein. Science, 223(4642), 1299-1301.

Oakley, A.J., Rossjohn, J., Lo Bello, M., Caccuri, A.M., Federici, G. and Parker, M.W., 1997. The three-dimensional structure of the human Pi class glutathione transferase P1-1 in complex with the inhibitor ethacrynic acid and its glutathione conjugate. Biochemistry, 36(3), 576-585.

Oakley, A.J., Lo Bello, M., Ricci, G., Federici, G. and Parker, M.W., 1998. Evidence for an induced-fit mechanism operating in pi class glutathione transferases. Biochemistry 37, 9912-9917.

Pace, C. N. (1986) Determination and analysis of urea and guanidine hydrochloride denaturation curves. Methods in Enzymology. 131, 266-280.

Pace, C.N., Vajdos, F., Fee, L., Grimsley, G. and Gray, T., 1995. How to measure and predict the molar absorption coefficient of a protein. Protein Science : A Publication of the Protein Society 4, 2411-2423.

Parker, J., 1989. Errors and alternatives in reading the universal genetic code. Microbiological Reviews, 53(3), 273.

Pettersen, E.F., Goddard, T.D., Huang, C.C., Couch, G.S., Greenblatt, D.M., Meng, E.C. and Ferrin, T.E., 2004. UCSF Chimera—a visualization system for exploratory research and analysis. Journal of Computational Chemistry, 25(13), 1605-1612.

Platz, E.A., and Giovannucci, E., 2004. The epidemiology of sex steroid hormones and their signaling and metabolic pathways in the etiology of prostate cancer. The Journal of Steroid Biochemistry and Molecular Biology, 92(4), 237-253.

Porath, J. and Flodin, P.E.R., 1959. Gel filtration: a method for desalting and group separation. Nature, 183(4676), 1657-1659.

Porath, J., 1992. Immobilized metal ion affinity chromatography. Protein Expression and Purification, 3(4), 263-281.

Prade, L., Huber, R., Manoharan, T.H., Fahl, W.E. and Reuter, W., 1997. Structures of class pi glutathione S-transferase from human placenta in complex with substrate, transition-state analogue and inhibitor. Structure (London, England : 1993) 5, 1287-1295.

Presta, L.G. and Rose, G.D., 1988. Helix signals in proteins. Science, 240(4859), 1632.

Privalov, P.L., 1979. Stability of proteins small globular proteins. Advances in Protein Chemistry, 33, 167-241.

Quesada-Soriano, I., Parker, L.J., Primavera, A., Casas-Solvas, J.M., Vargas-Berenguel, A., Baron, C., Morton, C.J., Mazzetti, A.P., Lo Bello, M., Parker, M.W. and Garcia-Fuentes, L., 2009. Influence of the H-site residue 108 on human glutathione transferase P1-1 ligand binding: structure-thermodynamic relationships and thermal stability. Protein Science : A Publication of the Protein Society 18, 2454-2470.

Ralat, L.A. and Colman, R.F., 2004. Glutathione S-transferase Pi has at least three distinguishable xenobiotic substrate sites close to its glutathione-binding site. The Journal of Biological Chemistry 279, 50204-50213.

Reed, M.C., Lieb, A. and Nijhout, H.F., 2010. The biological significance of substrate inhibition: a mechanism with diverse functions. BioEssays : News and Reviews in Molecular, Cellular and Developmental Biology 32, 422-429.

Reinemer, P., Dirr, H.W., Ladenstein, R., Huber, R., Lo Bello, M., Federici, G. and Parker, M.W., 1992. Three-dimensional structure of class pi glutathione S-transferase from human placenta in complex with S-hexylglutathione at 2.8 A resolution. Journal of Molecular Biology 227, 214-226.

Ricci, G., Bello, M.L., Caccuri, A.M., Pastore, A., Nuccetelli, M., Parker, M.W. and Federici, G., 1995. Site-directed Mutagenesis of Human Glutathione Transferase P1-1 Mutation Cys-47 induces a positive cooperativity in glutathione transferase P1-1. Journal of Biological Chemistry, 270(3), 1243-1248.

Richardson, J.S. and Richardson, D.C., 1988. Amino acid preferences for specific locations at the ends of alpha helices. Science, 240(4859), 1648.

Ries-Kautt, M.M. and Ducruix, A.F., 1989. Relative effectiveness of various ions on the solubility and crystal growth of lysozyme. Journal of Biological Chemistry 264, 745-748.

Roberts, D.D., Lewis, S.D., Ballou, D.P., Olson, S.T. and Shafer, J.A., 1986. Reactivity of small thiolate anions and cysteine-25 in papain toward methyl methanethiosulfonate. Biochemistry 25, 5595-5601.

Robinson, G.W., Robbins, R.J., Fleming, G.R., Morris, J.M., Knight, A.E.W. and Morrison, R.J.S., 1978. Picosecond studies of the fluorescence probe molecule 8-anilino-1-naphthalenesulfonic acid. Journal of the American Chemical Society, 100(23), 7145-7150.

Rosette, C. and Karin, M., 1996. Ultraviolet light and osmotic stress: activation of the JNK cascade through multiple growth factor and cytokine receptors. Science, 274(5290), 1194.

Rossjohn, J., Polekhina, G., Feil, S.C., Allocati, N., Masulli, M., Di Ilio, C. and Parker, M.W., 1998. A mixed disulfide bond in bacterial glutathione transferase: functional and evolutionary implications. Structure, 6(6), 721-734.

Rushmore, T.H., and Tony Kong, A., 2002. Pharmacogenomics, regulation and signaling pathways of phase I and II drug metabolizing enzymes. Current Drug Metabolism 3(5), 481-490.

Sau, A., Pellizzari Tregno, F., Valentino, F., Federici, G. and Caccuri, A.M., 2010. Glutathione transferases and development of new principles to overcome drug resistance. Archives of Biochemistry and Biophysics 500, 116-122.

Saxena, M., Singhal, S. S., Awasthi, S., Singh, S. V., Labelle, E. F., Zimniak, P. and Awasthi, Y. C., 1992. Dinitrophenyl S-glutathione ATPase purified from human muscle catalyses ATP hydrolysis in the presence of leukotrienes. Archives of Biochemistry and Biophysics 298, 231–237

Shea, T.C., Kelley, S.L. and Henner, W.D., 1988. Identification of an anionic form of glutathione transferase present in many human tumors and human tumor cell lines. Cancer Research, 48(3), 527-533.

Shimizu, T., Izumi, T., Honda, Z., Seyama, Y., Kurachi, Y. and Sugimoto, T., 1990. Biosynthesis and functions of leukotriene C4. Advances in Prostaglandin, Thromboxane, and Leukotriene Research, 20, 46-53.

Shishido, Y., Tomoike, F., Kimura, Y., Kuwata, K., Yano, T., Fukui, K., Fujikawa, H., Sekido, Y., Murakami-Tonami, Y., Kameda, T., Shuto, S. and Abe, H., 2017. A covalent G-site inhibitor for glutathione S-transferase Pi (GSTP1-1). Chemical Communications (Cambridge, England).

Shoichet, B.K., Baase, W.A., Kuroki, R. and Matthews, B.W., 1995. A relationship between protein stability and protein function. Proceedings of the National Academy of Sciences, 92(2), 452-456.

Simon, D.I., Mullins, M.E., Jia, L., Gaston, B., Singel, D.J. and Stamler, J.S., 1996. Polynitrosylated proteins: characterization, bioactivity, and functional consequences. Proceedings of the National Academy of Sciences, 93(10), 4736-4741.

Sinning, I., Kleywegt, G.J., Cowan, S.W., Reinemer, P., Dirr, H.W., Huber, R., Gilliland, G.L., Armstrong, R.N., Ji, X., Board, P.G. and Olin, B., 1993. Structure determination and refinement of human alpha class glutathione transferase A1-1, and a comparison with the Mu and Pi class enzymes. Journal of molecular biology, 232(1), pp.192-212.

Sneath, P.H.A. and Sokal, R.R., 1973. Numerical Taxonomy Freeman San Francisco.

Sreerama, N. and Woody, R.W., 2000. Estimation of protein secondary structure from circular dichroism spectra: comparison of CONTIN, SELCON, and CDSSTR methods with an expanded reference set. Analytical biochemistry 287, 252-260.

Stenberg, G., Abdalla, A.M. and Mannervik, B., 2000. Tyrosine 50 at the subunit interface of dimeric human glutathione transferase P1-1 is a structural key residue for modulating protein stability and catalytic function. Biochemical and Biophysical Research Communications, 271(1), 59-63.

Stenberg, G., Dragani, B., Cocco, R., Mannervik, B. and Aceto, A., 2000. A conserved "hydrophobic staple motif" plays a crucial role in the refolding of human glutathione transferase P1-1. Journal of Biological Chemistry, 275(14), 10421-10428.

Strange, R.C., Davis, B.A., Faulder, C.G., Cotton, W., Bain, A.D., Hopkinson, D.A. and Hume, R., 1985. The human glutathione S-transferases: developmental aspects of the GST1, GST2, and GST3 loci. Biochemical Genetics, 23(11), 1011-1028.

Stuehr, D.J., 1997. Structure-function aspects in the nitric oxide synthases. Annual Review of Pharmacology and Toxicology, 37(1), pp.339-359.

Szabo, A.G. and Rayner, D.M., 1980. Fluorescence decay of tryptophan conformers in aqueous solution. Journal of the American Chemical Society, 102(2), 554-563.

Takano, K., Ogasahara, K., Kaneda, H., Yamagata, Y., Fujii, S., Kanaya, E., Kikuchi, M., Oobatake, M. and Yutani, K., 1995. Contribution of hydrophobic residues to the stability of human lysozyme: calorimetric studies and X-ray structural analysis of the five isoleucine to valine mutants. Journal of Molecular Biology, 254(1), 62-76.

Takano, K., Yamagata, Y., Fujii, S. and Yutani, K., 1997. Contribution of the hydrophobic effect to the stability of human lysozyme: calorimetric studies and X-ray structural analyses of the nine valine to alanine mutants. Biochemistry, 36(4), 688-698.

Tanford, C., 1968. Protein denaturation. Advances in Protein Chemistry, 23, 121-282. Academic Press.

Teague, S.J., 2003. Implications of protein flexibility for drug discovery. Nature Reviews Drug Discovery, 2(7), 527.

Teale, F.W., 1960. The ultraviolet fluorescence of proteins in neutral solution. The Biochemical Journal 76, 381-388.

Tempfer, C.B., Schneeberger, C. and Huber, J.C., 2004. Applications of polymorphisms and pharmacogenomics in obstetrics and gynecology. Pharmacogenomics, 5(1), 57-65.

Terrier, P., Townsend, A.J., Coindre, J.M., Triche, T.J. and Cowan, K.H., 1990. An immunohistochemical study of pi class glutathione S-transferase expression in normal human tissue. The American Journal of Pathology, 137(4), p845.

Tew, K.D., Monks, A., Barone, L., Rosser, D., Akerman, G., Montali, J.A., Wheatley, J.B. and Schmidt, D.E., 1996. Glutathione-associated enzymes in the human cell lines of the National Cancer Institute Drug Screening Program. Molecular Pharmacology, 50(1), 149-159.

Tidefelt, U., Elmhorn-Rosenborg, A., Paul, C., Hao, X.Y., Mannervik, B. and Eriksson, L.C., 1992. Expression of glutathione transferase π as a predictor for treatment results at different stages of acute nonlymphoblastic leukemia. Cancer Research, 52(12), 3281-3285.

Townsend, D.M., Findlay, V.J., Fazilev, F., Ogle, M., Fraser, J., Saavedra, J.E., Ji, X., Keefer, L.K. and Tew, K.D., 2006. A glutathione S-transferase π-activated prodrug causes kinase activation concurrent with S-glutathionylation of proteins. Molecular Pharmacology, 69(2), 501-508.

Uchida, K., 2000. Induction of glutathione S-transferase by prostaglandins. Mechanisms of Ageing and Development, 116(2), 135-140.

Uhlén, M., Forsberg, G., Moks, T., Hartmanis, M. and Nilsson, B., 1992. Fusion proteins in biotechnology. Current Opinion in Biotechnology, 3(4), 363-369.

van der Kamp, M.W. and Mulholland, A.J., 2008. Computational enzymology: insight into biological catalysts from modelling. Natural Product Reports 25, 1001-1014.

Verghese, J., Abrams, J., Wang, Y. and Morano, K.A., 2012. Biology of the heat shock response and protein chaperones: budding yeast (Saccharomyces cerevisiae) as a model system. Microbiology and Molecular Biology Reviews : MMBR 76, 115-158.

Voehringer, D.W., Hirschberg, D.L., Xiao, J., Lu, Q., Roederer, M., Lock, C.B., Herzenberg L.A and Steinman, L., 2000. Gene microarray identification of redox and mitochondrial elements that control resistance or sensitivity to apoptosis. Proceedings of the National Academy of Sciences, 97(6), 2680-2685.

Wallace, L.A. and Dirr, H.W., 1999. Folding and assembly of dimeric human glutathione transferase A1-1. Biochemistry 38, 16686-16694.

Wang, X.Y., Zhang, Z.R. and Perrett, S., 2009. Characterization of the activity and folding of the glutathione transferase from Escherichia coli and the roles of residues Cys(10) and His(106). The Biochemical Journal 417, 55-64.

Watson, M.A., Stewart, R.K., Smith, G., Massey, T.E. and Bell, D.A., 1998. Human glutathione S-transferase P1 polymorphisms: relationship to lung tissue enzyme activity and population frequency distribution. Carcinogenesis 19, 275-280.

Waugh, D.S., 2005. Making the most of affinity tags. Trends in Biotechnology, 23(6), 316-320.

Weber, G. and Laurence, D.J., 1954. Fluorescent indicators of adsorption in aqueous solution and on the solid phase. The Biochemical Journal 56, xxxi.

West, M.B., Hill, B.G., Xuan, Y.T. and Bhatnagar, A., 2006. Protein glutathiolation by nitric oxide: an intracellular mechanism regulating redox protein modification. The FASEB Journal, 20(10), 1715-1717.

Whitmore, L. and Wallace, B.A., 2004. DICHROWEB, an online server for protein secondary structure analyses from circular dichroism spectroscopic data. Nucleic Acids Research 32, W668-673.

Whitmore, L. and Wallace, B.A., 2008. Protein secondary structure analyses from circular dichroism spectroscopy: methods and reference databases. Biopolymers, 89(5), 392-400.

Wilson, R.S., Khanal, A. and Bahnson, B., 2009. Peroxiredoxin VI in Complex With a Transition Inhibitor. The FASEB Journal, 23(1 Supplement), 504-8.

Woody, R.W., 1995. Circular dichroism. Methods in Enzymology 246, 34-71.

Yang Y., Cheng J.Z., Singhal S.S., Saini M., Pandya U., Awasthi S. and Awasthi Y.C., 2001. Role of glutathione S-transferases in protection against lipid peroxidation. Overexpression of hGSTA2-2 in K562 cells protects against hydrogen peroxide-induced apoptosis and inhibits JNK and caspase 3 activation. Journal of Biological Chemistry 276(22):19220-30

Yassin, Z., Ortiz-Salmeron, E., Garcia-Maroto, F., Baron, C. and Garcia-Fuentes, L., 2004. Implications of the ligandin binding site on the binding of non-substrate ligands to Schistosoma japonicum-glutathione transferase. Biochimica et biophysica acta 1698, 227-237.

Yin, Z., Ivanov, V.N., Habelhah, H., Tew, K. and Ronai, Z.E., 2000. Glutathione S-transferase p elicits protection against H_2O_2-induced cell death via coordinated regulation of stress kinases. Cancer Research, 60(15), 4053-4057.

Zimniak, P., Nanduri, B., Pikuła, S., Bandorowicz-Pikuła, J., Singhal, S.S., Srivastava, S.K., Awasthi, S. and Awasthi, Y.C., 1994. Naturally occurring human glutathione S-transferase GSTP1-1 isoforms with isoleucine and valine in position 104 differ in enzymic properties. The FEBS Journal, 224(3), 893-899.

Zuckerkandl, E. and Pauling, L., 1965. Evolutionary divergence and convergence in proteins. Evolving Genes and Proteins, 97, 97-166.

APPENDIX

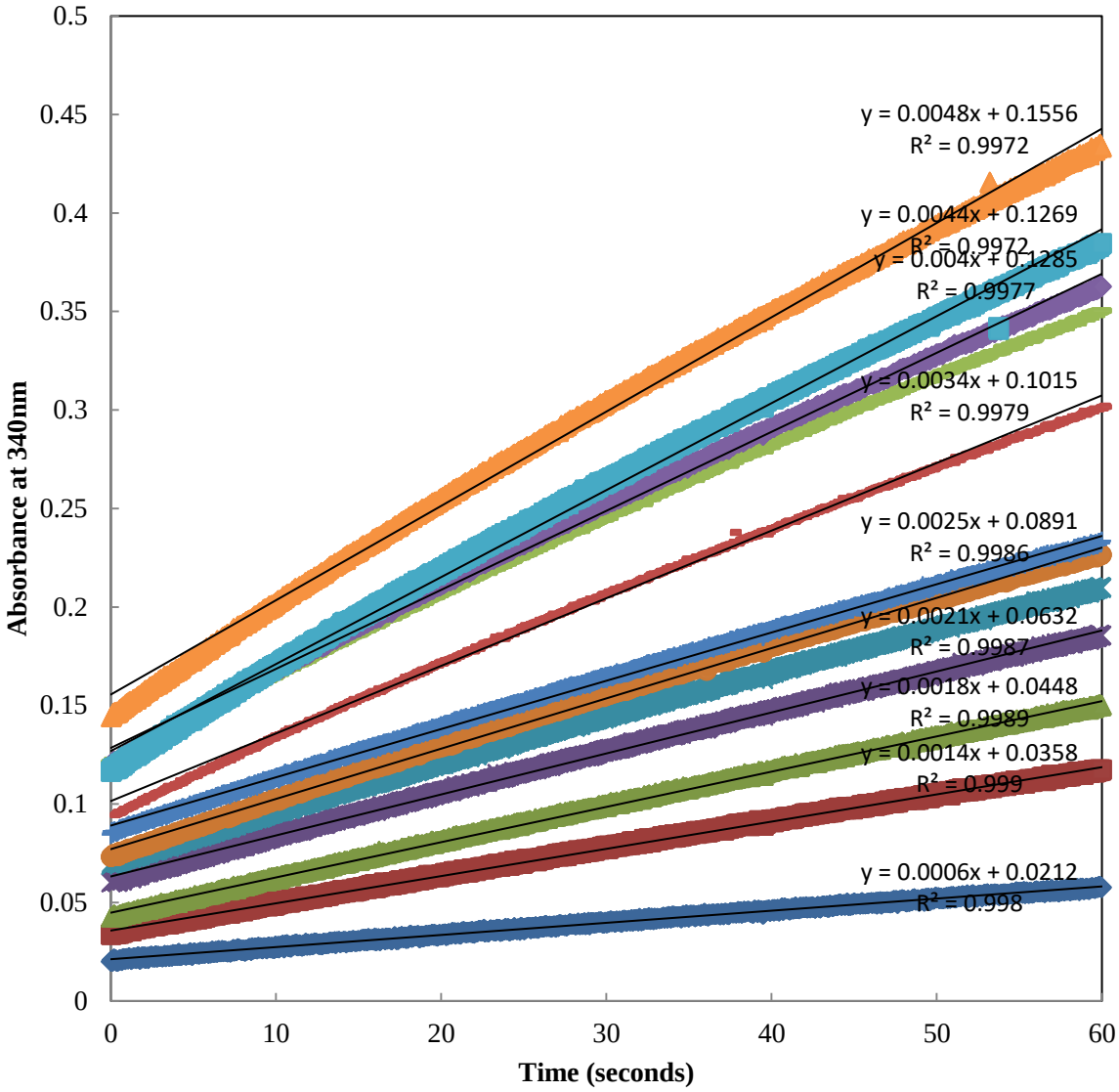

Figure A: Absorbance at 340 nm plotted as a function of time to determine the activity of GST-P1. The CDNB-GSH conjugation assay was done by mixing 1 mM CDNB, 1 mM GSH and increasing concentrations of protein. Progress curves for reactions with protein in them (6-28 nM) have been corrected for the blank (0 nM protein). All reactions were done at a pH of 6.5.

Table A: The initial parameters that were used to fit the intrinsic fluorescence and circular dichroism unfolding data to a two–state model for a dimeric protein (N2 → 2U) using the equation $f = F_U(y_u - y_n) + y_n$.

Parameter	Trp fluorescence	CD
m1	0.0125	10.327
m_n	0.0009	0.2765
m_u	0.0027	0.5613
y_n	0.9845	-21.278
y_u	1.0148	-6.8981